國立臺灣大學理學院海洋研究所

碩士論文

Institute of Oceanography

College of Science

National Taiwan University

Master Thesis

生活史特徵、氣候變遷與漁撈壓力對魚類族群的空間變異之影響

Influences of life-history traits, climate transitions and fishing on fish spatial dynamics

林哲越

Jhe-Yue Lin

指導教授: 謝志豪 博士

Advisor: Chih-hao Hsieh, Ph.D.

中華民國 112 年 6 月

June 2023

doi:10.6342/NTU202301753

國立臺灣大學碩士學位論文
口試委員會審定書
MASTER'S THESIS ACCEPTANCE CERTIFICATE
NATIONAL TAIWAN UNIVERSITY

生活史特徵、氣候變遷與漁撈壓力對魚類族群的空間變異之影響

Influences of life-history traits, climate transitions and fishing on fish spatial dynamics

本論文係林哲越 (R09241209)在國立臺灣大學海洋研究所完成之碩士學位論文，於民國 112 年 6 月 27 日承下列考試委員審查通過及口試及格，特此證明。

The undersigned, appointed by the Institute of Oceanography on 27 / 6 / 2023 have examined a Master's thesis entitled above presented by Jhe-Yue Lin (R09241209) candidate and hereby certify that it is worthy of acceptance.

口試委員 Oral examination committee:

謝志豪　張俊偉

（指導教授 Advisor）

張以杰　柯佳吟

系主任/所長 Director: 謝志豪

doi:10.6342/NTU202301753

誌謝

首先感謝若虞，這篇論文最大的推手，給予我研究上的指導與修正，何其有幸，能在求學生涯遇到妳，也相信妳未來能夠成為一位優秀的老師。

感謝俊偉，張老師，我的口委，督促我完成這篇論文，並點出我研究上的不足，願你的教學生涯一切順利。

感謝品嶧，我的學弟，因為你的加入，你的積極與熱情，為實驗室生活帶來不一樣的風采。

感謝承泰，我的學弟，也是我的快樂泉源，在我乏味的生活中，增添了不少歡笑，並參與我每一場演講，精神與我同在。

感謝曉航，陶老師，在研究上的支持與鼓勵，願你在法國一切平安順利。

最後感謝我的指導教授，謝老師，一再的包容，耐心地指導我的研究，並給予肯定，願老師能夠達成人生的所有目標。

希望之後看過這篇論文的每一位學生，這篇論文能帶給你幫助，帶給你啟發，也希望你們都能充實度過兩年碩士生涯，充滿嚮往地踏進台大，驕傲地，開開心心地離開校園。

doi:10.6342/NTU202301753

中文摘要

空間同步效應是指同一物種分散在不同區域的族群會有相似的豐度變化情形，是一種常見的族群時空動態特徵。空間同步效應的強度會受到內在(例如: 個體散布、密度調節及生活史特徵)和外在因素影響(例如: 環境因子和漁撈)而有所不同。了解這些內外在因素對於空間同步效應所造成的影響至關重要，因為空間同步效應的改變會影響重要生態過程及功能，例如物種滅絕危機、疾病傳播和食物生產。在這篇研究當中，我探討氣候變遷和漁撈作用對於魚類族群的空間同步效應之影響，並將魚種的生活史特徵納入考量。我分析加州沿近海 16 種受捕撈影響和 13 種沒有受捕撈影響的魚種、海表溫(SST)和風速的空間同步效應之情形(1951-2007)，資料取自 California Cooperative Oceanic Fisheries Investigations (CalCOFI)。我估算出各物種在空間距離為零之空間同步效應(ρ_0)，在跨物種分析上發現，隨著特定生活史數值(性成熟年齡、性成熟體長、最大體長及食物階層)的增加，ρ_0會有下降的情形，意味著 K 策略性的物種具有較低程度的空間同步效應。更重要的是，在考慮物種生活史特徵下，受捕撈影響物種相較於沒有受捕撈影響物種，具有較高的空間同步效應值(ρ_0)，顯示漁撈會對物種的空間同步效應造成影響。另一方面，氣候變遷也改變環境因子和魚種的空間同步效應。在分析中發現，海表溫、風速及六種中的四種呈現完整的同步效應隨距離衰減之魚種，在氣候暖期顯現出較高程度的空間同步效應，因此環境因子空間同步效應的上升可能是導致魚群空間同步效應上升的主因。這些結果顯示外部因素（例如，氣候

doi:10.6342/NTU202301753

變遷及漁撈)會導致物種空間同步效應增加,進而使物種產生不穩定的族群動態,可能導致滅絕危機的提升。結論顯示避免空間同步效應上升具有一定的必要性,這是維持族群動態穩定性及生物資源永續利用的關鍵因素。

關鍵字 : 空間同步效應；生活史特徵；氣候變遷；漁撈效應；族群動態穩定性

doi:10.6342/NTU202301753

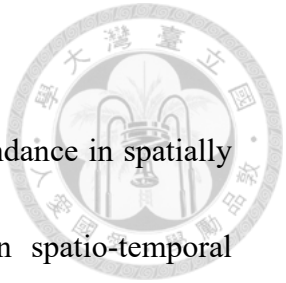

Abstract

Spatial synchrony, which refers to the simultaneous change of abundance in spatially separated subpopulations of a species, is a common feature in spatio-temporal population dynamics. The degree of spatial synchrony can be influenced by various intrinsic (e.g., dispersal, density regulation, and life-history traits) and extrinsic (e.g., environmental forcing and fishing) processes. Understanding the underlying mechanisms that drive such changes in spatial synchrony is essential because it can impact crucial ecological processes and functionings such as extinction risk, disease outbreak, and food production. In this study, I focus on investigating the response of spatial synchrony to climate transitions and fishing, with consideration of life-history traits of fish species. I extracted data from the California Cooperative Oceanic Fisheries Investigations (CalCOFI) spanning the years from 1951 to 2007. I analyzed data of 16 exploited and 13 unexploited fish species, as well as sea surface temperature (SST) and wind speed of the CalCOFI region. My findings revealed that, in general, spatial synchrony at distance approaching zero (ρ_0) decreases with certain increasing life-history traits (including age at maturation, length at maturation, maximum length, and trophic level). This finding indicates that species with traits associated with K-strategy tend to exhibit lower synchrony in nearby regions. Interestingly, exploited species demonstrated higher ρ_0 values compared to unexploited species, after accounting for

doi:10.6342/NTU202301753

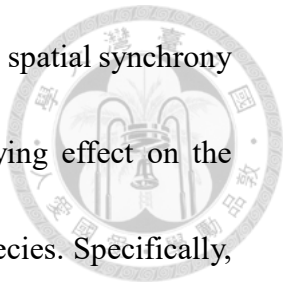

their life-history trait variation, suggesting that fishing has altered the spatial synchrony patterns of species. In addition, climate transitions have a modifying effect on the spatial synchrony of both environmental variables and some fish species. Specifically, during warm climate period, I observed an increase in synchrony for SST, wind speed, and four out of six species with the complete synchrony decay patterns. Thus, the increasing synchrony of environmental variables may be the underlying reason for the increasing synchrony observed among those fish species. My results emphasize that extrinsic factors such as climate transitions and fishing can enhance the spatial synchrony of fish, consequently leading to unstable population dynamics and an elevated risk of extinction. In order to maintain the stability of population dynamics and promote sustainable resource utilization, it is crucial to prevent the occurrence of strong spatial synchrony among subpopulation for a species.

Keyword : Spatial synchrony, Life-history traits, Climate transitions, Fishing, Population dynamics stability

doi:10.6342/NTU202301753

Table of contents

doi:10.6342/NTU202301753

List of Figures

doi:10.6342/NTU202301753

List of tables

doi:10.6342/NTU202301753

Introduction

Fish populations exhibit high variability over time and space, and these variations in abundance are influenced by both intrinsic (e.g., demographic processes such as birth, migration and death) and extrinsic processes (e.g., stochastic environmental events and harvesting). Understanding the underlying mechanisms driving such spatio-temporal dynamics is a central focus in population ecology and fisheries science, due to their impacts on ecological processes and resource management (Adams et al., 2018; Bell et al., 2015; Engelhard et al., 2014).

Spatial synchrony, which refers to similar abundance fluctuations occurring simultaneously among spatially separated subpopulations of the same species (Liebhold et al., 2004), is a common feature in spatio-temporal population dynamics. This phenomenon has been observed in various species and taxa (Defriez et al., 2016; Jared et al., 2015; Pardikes et al., 2017; Post & Forchhammer, 2004). Generally, spatial synchrony decreases as the distance between subpopulations increases (Lande et al., 1999; Myers et al., 1997; Ranta et al., 1995), and the shape of this decline determines the strength and scale of synchrony process (Engen et al., 2002). Moreover, the shape of decline can be used to infer the cause of synchrony (Jared et al., 2015; Nicolau et al., 2022). Spatial synchrony can arise from both intrinsic and extrinsic processes. For example, intrinsic

doi:10.6342/NTU202301753

processes such as dispersal of individuals can couple similar abundance fluctuations among spatially separated subpopulations (Paradis et al., 1999). Extrinsic processes such as predator-prey interaction, e.g., predator can regulate prey populations synchronously across different locations (Krebs et al., 2001), and spatially correlated environmental events (e.g., successive temperature, wind speed, and rainfall events) can also synchronize abundance fluctuations (Engen et al., 2005; Grøtan et al., 2005; Jared et al., 2015; Lande et al., 1999). This environment-driven synchrony is known as the "Moran effect" (Moran, 1953). Additionally, other factors have also been observed to cause spatial synchrony such as geography and habitat type (Frank et al., 2016; Paradis et al., 2000; Walter et al., 2017). However, it is challenging to disentangle the relative contributions of these factors because they often interact with each other and simultaneously influence spatially separated subpopulations of a species.

Marine environments are undergoing changes due to climate change. Anomalous environmental events such as rising water temperature, ocean circulation changes, intensified stratification and acidification, have become ubiquitous, increasing in occurrence and duration synchronously across regions (Di Cecco & Gouhier, 2018; Wang et al., 2015; Wu et al., 2012). These events transform marine environment from a complex heterogeneous pattern to a simple homogeneous pattern. Homogeneous, unfavorable

doi:10.6342/NTU202301753

environmental conditions profoundly influence physical responses, geographic distribution, and abundance fluctuation of marine organisms (Perry et al., 2005; Stuart-Smith, 2021; Wang et al., 2020), thereby weakening their resilience to natural and anthropogenic disturbances. Furthermore, climate change-promoted homogeneity in environment is known to regulate population spatial synchrony, particularly on a large spatial scale. According to the "Moran effect", the spatial synchrony of environment will lead to the spatial synchrony of the population (Moran, 1953). Consequently, as environmental synchrony increases, perhaps due to climate change, the strength of spatial synchrony among subpopulations can also be magnified, as observed in theoretical and empirical studies (Koenig & Liebhold, 2016; Post & Forchhammer, 2004; Sheppard et al., 2016). For instance, in the western Greenland, large-scale warming caused an increase in spatial synchrony among caribou subpopulations, potentially enhancing their risk of extinction, once subpopulations all experience declines in abundance at the same time (Post & Forchhammer, 2004).

Spatial synchrony has generally been viewed to arise from natural events. However, human activities such as fishing may also contribute to synchronous abundance fluctuations. Fishing is the most widespread anthropogenic disturbance in the ocean and has become a major threat to populations and communities. With increasing scale and

doi:10.6342/NTU202301753

development, fishing can operate independently of time and space, simultaneously regulating population abundance across different regions. For example, in the North Atlantic, the rise and fall of cod abundance were driven by commercial fisheries, and these harvesting-induced fluctuations could extend over thousands of kilometers, which is comparable to the scale of climate effects (Frank et al., 2016). Apart from directly regulating population size, fishing is a selective process that primarily targets larger or older individuals in the population. Different age classes of fish contribute differently to spatial synchrony patterns, with older age classes having more contributions than younger age classes (Marquez et al., 2021). Thus, the removal of older age classes might modify species' spatial synchrony patterns. Theoretical studies have also predicted that specific harvesting strategies, such as selective harvesting, could enhance the strength of spatial synchrony (Engen et al., 2018). These results highlight the need to avoid harvest-promoted synchrony over large areas as it can have detrimental effects on fishery industries (Oken et al., 2021), and increase the risk of species extinction (Brown & Kodric-Brown, 1977; Earn et al., 2000).

Spatial synchrony varies among species with different life histories (Marquez et al., 2019). Life-history traits can modulate a species' spatial synchrony pattern through demographic variables such as generation time, fecundity, and colonization. For instance,

doi:10.6342/NTU202301753

species with slow life-history traits (e.g., long lifespan, slow growth rate, and late sexual maturation) tend to have a longer scaling of spatial synchrony (the range that spatial synchrony occur), compared to species with fast life-history traits (Marquez et al., 2019). Because slow life-history species have weaker strength of density dependence and better dispersal and colonization ability, which allow them to disperse and spread synchronous fluctuations across regions (Marquez et al., 2019). This finding is consistent with the study by Kuo et al. (2016), which showed that K-selected species have a more homogeneous spatial distribution pattern, thereby coupling similar dynamics pattern among subpopulations. Furthermore, ecological traits, such as geographic affinity (e.g. preference in cold water, warm water, or eurytherm) and habitat preferences, may also affect spatial synchrony patterns (Hsieh et al., 2009). For example, dense vegetation in a habitat can limit individual movement and communication, thereby reducing synchrony among subpopulations (Paradis et al., 1999). Understanding these species-specific spatial synchrony patterns is crucial for management and conservation efforts (Marquez et al., 2019).

Based on previous and recent studies, there is a critical need for study that incorporates life-history traits, climate variations, and fishing to gain a fundamental understanding of how spatio-temporal dynamics respond to intrinsic and extrinsic processes. Because

doi:10.6342/NTU202301753

spatial synchrony can have significant implications for crucial ecological processes and functionings, such as extinction risk of metapopulations (Engen et al., 2002; Stowe et al., 2020; Sutherland et al., 2012), disease outbreaks (Sheppard et al., 2016), and food production (Oken et al., 2021). However, most of the studies focused on either life-history traits, climate change or fishing along, and no study to date has examined these three effects on spatial synchrony. In this study, I utilized a long-term dataset from the California Cooperative Oceanic Fisheries Investigations (CalCOFI) scientific trawl survey to investigate the effects of climate transitions and fishing on spatial synchrony of 29 fish species. I also considered life-history and ecological traits known to influence population responses to intrinsic and extrinsic mechanisms. I aimed to address the following three questions: (1) Is there a relationship between life-history traits and spatial synchrony? (2) Does increasing environmental synchrony follow with increasing population synchrony during climate transitions? (3) Does fishing modify the strength of spatial synchrony in exploited species, in comparison with the unexploited species?

doi:10.6342/NTU202301753

Methods and Materials

Data

To commence this study, I extracted long-term abundance and distribution data of 29 dominant coastal-neritic larval fish species (1951-2007) (Table S1) from the California the Cooperative Oceanic Fisheries Investigations (CalCOFI) scientific larval fish survey conducted in the southern California Current Ecosystem. Since most larvae were collected in early life stages, their abundances and distributions were considered as proxies for the biomasses and locations of their spawning stocks (Hsieh et al., 2008; Hsieh et al., 2006). To identify the principal spawning areas for each species, I only included the sampling stations with at least three non-zero density records. By utilizing these selected stations, I constructed convex hulls to represent the principal spawning areas of each species (Figure S2) (Kuo et al., 2016). Additionally, I restricted my analysis to data collected during the defined spawning season, as described in Hsieh et al. (2006). The sampling frequency of the CalCOFI survey was not consistent over time, but quarterly sampling was conducted in each year. Therefore, I utilized quarterly data to avoid bias in the estimation of spatial synchrony (Hsieh et al., 2005; Kuo et al., 2016). Among the 29 fish species, 16 were classified as exploited species and 13 as unexploited species (Table S2) (Hsieh et al., 2006). I considered their life-history traits, including age at 50% maturation, length at 50% maturation, maximum length, trophic level, fecundity, and spawning duration (Table S1) (Hsieh et al., 2006; Kuo et al., 2016). I also took into

doi:10.6342/NTU202301753

account ecological traits of the species, including habitat, geographic affinities, and spawning mode (Table S3) (Hsieh et al., 2006).

To examine the environmental effects on spatial synchrony, I utilized sea surface temperature (SST) and wind speed data obtained from the CalCOFI hydrographic survey. SST is considered an important indicator of climate conditions and can reflect temporal climate variations. Wind speed is known to influence current advection, which in turn affects the distribution and dispersal of larval fish (Defriez et al., 2016; Hsieh et al., 2008; Sheppard et al., 2019).

Estimation of spatial synchrony

In this study, the fish densities (Y) were log-transformed to ensure normality (Marquez et al., 2021). Then, density values of each station were standardized across the years (Marquez et al., 2021). After the standardization, I could write $Y \sim N(m, \sigma)$, where $mean \quad m = 0$, $standard \ deviation \quad \sigma = 1$. The fish densities (Y) were considered as a p-dimensional multivariate Gaussian random field $\mathrm{Y} = Y(s_1, t_1)$, $Y(s_2, t_2), \ldots, Y(s_n, t_n)'$, $\{Y(s,t), (s,t) \in \mathbb{R}^d, d \geq 1\}$, where s_n is the sampling station and *t* represents the year (Sherman, 2011). A general spatio-temporal model was used to describe the multivariate variables (Cressie & Wikle, 2015; Sherman, 2011; Zhang et al., 2015), given by Equation (1)

doi:10.6342/NTU202301753

$$Y(s,t) = \kappa(s) + W(s,t) + \varepsilon(s,t) \quad (1)$$

In Equation (1), $\kappa(s)$ represents the deterministic mean function, $W(s,t)$ is a zero-mean Gaussian process that represents spatially correlated variation from the mean, and $\varepsilon(s,t)$ is the Gaussian white noise process, representing local variation and sampling variability. The spatial dependence structure of $W(s,t)$ were detected using a covariance function C_w by Equation (2) below (Cressie & Wikle, 2015; Sherman, 2011; Zhang et al., 2015), describing the way that abundance variations W covary with separate distance (*d*)

$$C_w(d) = Cov\big(W(s_1,t), W(s_2,t)\big) = \sigma(s_1)\sigma(s_2)\rho_Y(d) \quad (2)$$

Because multivariate Gaussian random field has constant mean and variance, it is reasonable to assume that variance is equal among stations, $\sigma(s_1) = \sigma(s_2) = \sigma$ (Sang & Huang, 2012), then the covariance function expresses as

$$C_w(d) = \sigma^2\rho_Y(d) + \sigma_\varepsilon^2 \quad (3)$$

σ_ε^2 represents the error variance. Notably, I assume the sampling field to be isotropic, meaning that the covariance only depends on separate distance and not on separate

doi:10.6342/NTU202301753

direction (BjØrnstad & Falck, 2001). The spatial synchrony function ρ is derived from the covariance function and is defined by Equation (3) (Engen et al., 2005; Grøtan et al., 2005)

$$\rho(d) = \rho_\infty + (\rho_0 - \rho_\infty)e^{(-\frac{d^2}{2l^2})} \quad (4)$$

As described in Marquez et al. (2021), ρ_0 and ρ_∞ represents the correlation of abundance at the distance approaching zero and infinity, respectively. More specifically, ρ_0 is spatial synchrony process at the origin; the higher values at the origin, the more synchrony on the neighboring subpopulations will have on prediction. In contrast, ρ_∞ represents when spatial synchrony reaches the end, beyond which, generally, no synchrony occurs among spatially-distant subpopulations; but if subpopulations still show certain degree of synchrony, meaning that some kinds of large-scale process are affecting entire populations. In addition, $\exp(-\frac{d^2}{2l^2})$ is an exponential Gaussian decay function, describing how the correlation decays with increasing distance, where l represents the scaling of the spatial synchrony process, defined as the distance where abundances of subpopulations regarded as highly correlated. A higher value of l indicates a slower rate of decay with distance (Marquez et al., 2021).

To estimate the three spatial synchrony parameters ρ_0, ρ_∞, and l, I assumed all

doi:10.6342/NTU202301753

abundance variations W and error terms ε are normally distributed (Marquez et al., 2019), and the $W(s_1,t), W(s_2,t), \ldots W(s_{n_s},t)$ should follow multivariate normal distribution, with zero means and variance $\sum + \sigma_\varepsilon^2$, where $\sum$ is defined by $Cov\big(W(s_1,t), W(s_2,t)\big)$), as shown in Equation (4)

$$Y_t - \hat{k} \sim MVN(0, \sum + \sigma_\varepsilon^2) \quad (5)$$

In Equation (4), $\hat{k}$ is the vector of mean abundance at each station. $Y_t - \hat{k}$ is the W. After each element in the MVN is defined, the likelihood function can be completely specified (Marquez et al., 2019; Marquez et al., 2021), describing in Equation (5)

$$L\big(Y_t - \hat{k}; \theta\big) = \prod_{t=1}^{T} f(Y_t - \hat{k}|\theta) \quad (3)$$

θ is the vector of spatial synchrony parameters. By utilizing the likelihood function, numerical optimization techniques can be applied to estimate the spatial synchrony parameters (Marquez et al., 2019; Marquez et al., 2021). Parametric bootstrapping was used to generate the distribution of the three parameters (Engen et al., 2005; Grøtan et al., 2005; Marquez et al., 2021). This involved resampling the abundance vector Y_t with replacement for 500 iterations and fitting the spatial synchrony function to each resample dataset. Ultimately, the spatial synchrony parameters for each species were the median

doi:10.6342/NTU202301753

values that obtained from bootstrapping estimation (Marquez et al., 2019; Marquez et al., 2021).

Spatial synchrony under influences of life-history traits, climate transitions and fishing

Weighted least square regressions were used to examine the relationship between each of the life-history traits and spatial synchrony parameters. This approach could account for the error variance that generated from the parameter estimations. Furthermore, the regressions were additionally conducted on exploited and unexploited species independently; as such, I can detect the effect of fishing from the two species categories.

When estimating the spatial synchrony parameters for each species, there were high uncertainties appeared in the bootstrapping results. These high uncertainties resulted from the species with incomplete synchrony decay patterns (e.g., non-significant decay synchrony). To address these issues, the following steps were implemented to determine complete and incomplete synchrony decay patterns for each species:

1. The number of occurring stations was required to be larger than 30, following the similar concept used in variogram analysis, which is a common method in geostatistics when conducting observation-pair comparisons (Buelga Díaz et al., 2022). This criterion ensured a sufficient dataset for reliable estimation of spatial

doi:10.6342/NTU202301753

synchrony and effectively prevented high uncertainty conditions.

2. Differences between the lower bound of the initial distance and upper bound of the maximum distance were calculated from the 95% confidence interval for each species. If the difference was positive, it indicated a complete synchrony decay pattern.

After identifying the species with complete synchrony decay pattern, I selected those species to examine their spatial synchrony patterns during climate transitions. A climate transition occurred in the southern California Current region, shifting from a cold to a warm climate phase. The cold climate period spanned from 1951 to 1976, while the warm climate period occurred from 1977 to 1998 (Hsieh et al., 2008). Spatial synchrony of environmental variables and fishes was measured separately during the cold and warm climate periods. Additionally, I also examined spatial synchrony patterns of exploited and unexploited species during these two climate periods to explore whether there were differences between species groups.

The estimation of spatial scaling l showed extremely large values in the results, suggesting synchrony did not decrease with increasing distance. To facilitate comparison between different categories, the spatial scaling values were transformed into a decay function γ by taking the logarithm to the exponential part that controls the decay rate

doi:10.6342/NTU202301753

$(-\log(\frac{1}{2l}))$ (Marquez et al., 2019). This transformation allowed for a more meaningful comparison between species.

doi:10.6342/NTU202301753

Results

Spatial synchrony of fishes

The analysis of spatial synchrony among 29 fish species revealed substantial variations, as depicted in Figure S1. The spatial synchrony patterns were influenced by the correlations between station pairs, with the quantity and distribution of correlation points determining how synchrony (ρ) changed with increasing distance. Notably, negative correlations (asynchronous abundance fluctuations) were replaced by zero in the analysis. On the one hand, some species exhibited high spatial synchrony pattern, such as Northern anchovy and Pacific sardine (Figure S1 (4, 18)). That is, these species displayed high synchrony at the beginning (when distance approached zero), and as distance increased, synchrony remained at a certain level (around 25%). On the other hand, several species showed low spatial synchrony patterns, e.g., California smoothtongue and Jack mackerel (Figure S1 (8, 28)). Synchrony for these species is close to zero across all distances. Due to limitations in the dataset, most species exhibited relatively incomplete spatial synchrony patterns. For some species, synchrony patterns abruptly ceased at a certain distance (e.g., Pacific argentine, Blacksmith and Bigmouth sole; Figure S1 (1, 2, and 5)), whereas others showed no changes in synchrony as distance increased, resulting in a straight line pattern (e.g., Medusafish, slender sole and Shortbelly rockfish; Figure S1 (7, 9, and 22)). When selecting only the species with a sufficient number of occurring stations (larger than 30), as shown in Figure 1, the results became clearer, although some species

doi:10.6342/NTU202301753

still did not exhibit the typical pattern of synchrony decreasing with increasing distance. Finally, by analyzing the differences between the lower bound and upper bound values from the confidence interval, species with complete synchrony decay patterns were identified (grey background in Figure 1). Only six species demonstrated complete synchrony decay pattern, including five exploited species (northern anchovy, Pacific hake, Pacific sardine, Pacific chub mackerel, and Jack mackerel; Figure 1 (a), (e), (f), (g), (m)) and one unexploited species (California smoothtongue; Figure 1 (c)).

Estimation of spatial synchrony parameters

The estimation of spatial synchrony at distance approaching zero (ρ_0) was possible for all species (regardless whether the synchrony pattern is complete or not), and the estimations were relatively stable compared to the other parameters, as shown in Table 1. Certainly, species with complete synchrony decay patterns had more reliable ρ_0 estimations, as indicated by the narrower confidence intervals. In contrast, the results of spatial synchrony at distance approaching infinite (ρ_∞) and spatial scaling (l) exhibited high uncertainties or could not be estimated for most species, except for those with complete synchrony decay patterns (Table 2, Table 3). It is common for ρ_∞ to approach zero in most cases, indicating that there is no synchrony among spatially-distant subpopulations. However, some species still showed a certain degree of synchrony even at long distances. From the spatial scaling l results, several species show extremely large

doi:10.6342/NTU202301753

scaling values (Table 3). Those extreme values were due to the incomplete synchrony decay pattern, suggesting synchrony did not decay with increasing distance. But after the log-transformation, the decay function γ were more reasonable to make the comparison (Table 4).

Spatial synchrony parameters versus life-history traits

As shown in Figure 2, there is a negative relationship between certain life-history traits and the spatial synchrony parameters ρ_0. Specifically, age at maturation, length at maturation, maximum length, and trophic level exhibit a negative association with ρ_0. Only age at maturation and trophic level demonstrate a statistically significant linear relationship ($p < 0.05$). However, fecundity and spawning duration demonstrate positive relationship with ρ_0. In contrast, the plots of ρ_∞ and l versus life-history traits are limited by the species with incomplete synchrony decay patterns (Figure S3; Figure S4), represented by open diamonds in the plots. As a result, no significant linear relationship is observed between these life-history traits and the spatial synchrony parameters ρ_∞ and l. The high uncertainties and incomplete synchrony patterns make it challenging to establish meaningful relationship between these variables. Overall, most life-history traits exhibit a negative relationship with the spatial synchrony parameter ρ_0, while the relationships with ρ_∞ and l are less conclusive due to the limitations imposed by

doi:10.6342/NTU202301753

incomplete synchrony patterns.

Spatial synchrony during climate transitions

The plots of spatial synchrony between the cold climate period (1951-1976) and warm climate period (1977-1998) provide insights into how synchrony changes over time (Figure 3; Figure 4). Both environmental variables, sea surface temperature (SST) and wind speed, exhibit an increase in spatial synchrony during the warm climate period (Figure 3). Although the increase in synchrony for wind speed is not as pronounced, it generally shows an upward trend, particularly at longer distances. For this analysis, only species with complete synchrony decay patterns (six species) were considered, as they have sufficient data for estimating synchrony between the two periods (Figure 4). Four fish species, namely California smoothtongue, Pacific hake, Pacific sardine and Jack mackerel, show a consistent pattern of increasing synchrony during the warm climate period (Figure 4 b, c, d, and f). The increasing synchrony for California smoothtongue and Pacific hake may not be apparent at shorter distances but becomes more prominent at distances of 200-400 km (Figure 4 b and c). In contrast, northern anchovy and Pacific chub mackerel exhibit a decrease in synchrony during the warm climate period (Figure 4 a and e). Furthermore, by examining the spatial-specific synchrony diagrams (Figure 5), it is possible to observe how spatial synchrony increased in the warm climate period. The

doi:10.6342/NTU202301753

diagrams illustrate pairs of stations connected by lines with different colors, representing the degree of spatial synchrony across space. In the cold climate period, strong synchrony is primarily observed in nearby areas (Figure 5 b(1), c(1), d(1), f(1)). However, in the warm climate period, strong synchrony extends to more distant regions, indicating synchronous abundance fluctuations occur over a broader scale (Figure 5 b(2), c(2), d(2), f(2)).

Spatial synchrony under fishing effects

The impact of fishing on species' spatial synchrony patterns is evident, as demonstrated by the differences between exploited and unexploited species (Figure 6). Exploited species exhibit higher spatial synchrony (ρ_0) compared to unexploited species when considering all life-history traits. In addition, the spatial synchrony at distance approaching zero (ρ_0) of exploited species shows a significant linear relationship with age at maturation ($\mathrm{r} = -0.54, \mathrm{p} = 0.05$), length at maturation ($\mathrm{r} = -0.55, \mathrm{p} = 0.049$), maximum length ($\mathrm{r} = -0.55, \mathrm{p} = 0.049$), and trophic level ($\mathrm{r} = -0.8, \mathrm{p} = 0.001$) (Figure 6 a, b, c, and d). However, ρ_0 of the unexploited species does not exhibit a significant linear relationship with any of the life-history traits. The results of ρ_∞ and l versus life-history traits for exploited and unexploited species do not provide useful information due to the high uncertainties in parameter estimation (Figure S5; Figure S6).

doi:10.6342/NTU202301753

Spatial synchrony versus ecological traits

It is observed that all species with a complete synchrony decay pattern belongs to open water species (Figure 7). Specifically, exploited species inhabiting open water habitats and exhibiting a complete synchrony decay pattern have higher ρ_0 and ρ_∞ vales compared to species in the other habitats. In terms of geographic region category (Figure 8), no specific pattern is evident among ρ_0, ρ_∞ and l. When considering the spawning mode, species with a complete synchrony decay pattern are all planktonic spawners (Figure 9). Moreover, exploited species that are planktonic spawners tend to have higher ρ_0 and ρ_∞ values compared to species with other spawning modes. However, no distinct pattern can be observed in the decay function (γ) for any of the ecological traits (Figure 7 - 9).

Spatial synchrony of exploited and unexploited species during climate transitions

The analysis of spatial synchrony versus life-history traits in cold and warm climate periods reveals no clear differences between the two periods (Figure S7; Figure S8). Exploited species exhibit a negative relationship between ρ_0 and life-history traits, consistent with the overall findings (Figure S7; Figure S8). However, the statistically

doi:10.6342/NTU202301753

significant patterns disappear in the warm period (Figure S8), except for trophic level. In comparison, unexploited species do not show any negative linear relationship between ρ_0 and life-history traits (Figure S7; Figure S8).

doi:10.6342/NTU202301753

Discussion

My results indicate that both climate transitions and fishing have increased the spatial synchrony of fish populations. During the warm climate period, influenced by the climate change-promoted homogeneity in environment (Figure 3), four of six species with complete synchrony decay patterns show increasing spatial synchrony patterns (Figure 4 b, c, d, and f). Interestingly, under the influence of fishing activities, exploited species exhibit higher spatial synchrony values (ρ_0) compared to unexploited species, after accounting for their life-history traits (Figure 6). These increasing synchrony patterns suggest that environmental variations and anthropogenic disturbance not only affect species' spatial or temporal dynamics (Hsieh et al., 2008; Hsieh et al., 2006; Kuo et al., 2016), but also spatio-temporal population dynamics. Exploring how spatial synchrony responds to those intrinsic and extrinsic processes can provide important applications in conservation and management (Stowe et al., 2020), because it can serve as an important indicator related to stability and persistence of population dynamics (Figure S11).

The pattern of spatial synchrony varies among the 29 fish species in this study (Figure S1), which can be attributed to their different life-history and ecological traits. Factors such as dispersal ability (Kuo et al., 2016), density regulation (Lande et al., 1999), trophic interactions (Krebs et al., 2001), habitat type (Myers et al., 1997), and environmental

doi:10.6342/NTU202301753

response (Marquez et al., 2019; Marquez et al., 2021), can influence the processes that regulate spatial synchrony (Figure 2, 7 - 9). For example, small pelagic fish species, such as northern anchovy and Pacific sardine, known for their schooling behavior and aggregation tendencies, exhibit strong dispersal effects that result in high spatial synchrony across all distance ranges (Figure 1 (a), (f)). In contrast, species like California smoothtongue, Pacific hake, Pacific chub mackerel, and Jack mackerel show lower spatial synchrony at longer distances (Figure 1 (c), (e), (g), (m)), possibly due to their lower aggregation tendencies or their occurrence in deeper water regions that hinder the ability of communication among individuals.

Incomplete synchrony decay patterns were observed in the majority of the species we examined, where synchrony suddenly ceases at a certain distance or remains constant with increasing distance (Figure S1). This may be attributed to several issues during the estimation process. Firstly, not having enough appearance stations can cause high uncertainty in spatial synchrony estimation. Because about half of the species we examined belong to nearshore species, meaning that they tend to aggregate in coastal areas, with limiting appearance station number that restricts the completeness of estimation (Figure S2; e.g., (1), (2), (5), (6), (12)). Secondly, abundance time series for some species show great variations across space, the non-overlapping time series between

doi:10.6342/NTU202301753

stations can lead to unreliable estimation of synchrony values, which are the cases in this study. Lastly, CalCOFI scientific survey encloses a relatively small sampling area compared to other studies (Marquez et al., 2019; Myers et al., 1997); this may also restrict the ability to fully capture the spatial synchrony patterns of widely distributed species.

The results in this study reveal a generally negative relationship between life-history traits and spatial synchrony at distance approaching zero ρ_0 (Figure 2; Figure 6). In particularly, no study ever examines the relationship between these two variables. In order to make the comparison between species with different life-history values, R/K selection is introduced here (Kuo et al., 2016). K-selected strategy refers to species that are larger size, have slower growth rate, and later sexual maturation (i.e., species with higher life-history trait values). In contrast, R-selected species are those having smaller size, faster growth rate, and younger sexual maturation individuals (i.e., species with lower life-history trait values). According to my results (Figure 2; Figure 6), species with K-selected traits (higher life-history values) have lower ρ_0 values. This may be attributed to a fundamental survival strategy that prevents cannibalism from happening, because predator and prey interaction is also one of the drivers that cause spatial synchrony (Krebs et al., 2001). To prevent the occurrence of cannibalism, different age classes (or size classes) often choose to live in different habitats (known as “ontogenetic shift”), showing

doi:10.6342/NTU202301753

segregation in spatial distribution (Pan et al., 2021), thereby reducing predation synchrony. On the contrary, R-selected species (lower life-history trait values) have higher ρ_0, which is reasonable and may be due to their aggregated behavior (Kuo et al., 2016), coupling similar dynamics among subpopulations.

During climate transitions, environmental variables such as SST and wind speed exhibit increasing spatial synchrony in the warm climate period (Figure 3). This increasing synchrony is also observed in four fish species with complete synchrony decay patterns, including California smoothtongue, Pacific hake, Pacific sardine and Jack mackerel (Figure 4 b, c, d, f). These findings suggest that the increasing spatial synchrony of fish populations may be driven by the increasing synchrony of environmental variables, aligning with the concept of the "Moran effect" where climate-induced environmental changes can synchronize population dynamics (Post & Forchhammer, 2004; Sheppard et al., 2016). California smoothtongue and Pacific hake showed less apparent increasing pattern (Figure 4 b, c). Considering that the influence of environmental factors often can reach more distant range (Post & Forchhammer, 2002), we find that both species showed increasing synchrony at longer distance (over 200 km, color bar below). In addition, the increasing patterns also differ among species. Pacific sardine showed more apparent enhancement than other species (Figure 4 d), which may due to its' susceptibility to

doi:10.6342/NTU202301753

environmental variations (Lindegren & Checkley Jr, 2013; Petatán-Ramírez et al., 2019), resulting in strong response to changing environmental synchrony. The synchronous abundance fluctuations in these species extend from nearby areas to more distant regions, indicating the expansion of similar dynamics across broader spatial scales (Figure 5 b(2), c(2), d(2), f(2)). However, northern anchovy and Pacific chub mackerel do not show the increasing synchrony pattern in the warm climate period (Figure 4 a, e). Those species' synchrony pattern may be influenced by other factors that mitigate the environmental effects. Ultimately, homogeneous environmental conditions not only lead to consistent change in abundance among spatially-separated subpopulations (Figure S9), but also may expand similar dynamics to broader regions in the CalCOFI survey area (Figure 5).

Exploited species show higher spatial synchrony ρ_0 than those for unexploited species, after accounting for life-history traits (Figure 6). This enhancement in synchrony may be attributed to the selective nature of fishing (Garcia et al., 2012; Hsieh et al., 2006), which primarily targets larger and older individuals of a population that contribute significantly to affecting spatial synchrony patterns (Marquez et al., 2021). Removing these larger and older individuals from the population can modify the spatial synchrony of the species. Because larger and older fish have better fitness and resistance to environmental stochasticity, and ability to find proper spawning grounds (Berkeley et al., 2004; Hixon

doi:10.6342/NTU202301753

et al., 2014; Planque et al., 2010). More importantly, those characteristics can pass on smaller and younger classes through vertical social learning (Huse et al., 2010). Consequently, larger and older individuals play an important role in maintaining population dynamics stability, and thus, they can reduce the degree of synchrony among spatially-separated subpopulations. My result of increasing spatial synchrony in exploited species is also in accordance with Hsieh et al. (2006). By using the same CalCOFI dataset, their results showed that fishing enhances abundance variability in exploited species. Strong spatial synchrony among subpopulations of the species can increase its' total abundance variation, because if abundance of subpopulations increased or decreased synchronously, their total abundance would show dramatically increase or decrease at the same time, and end up showing high temporal variability in abundance (Figure S10).

Increasing spatial synchrony can have serious consequences for both spatially separated subpopulations and whole metapopulation of a species. On the one hand, strong synchrony can erode the "spatial rescue effect" (Earn et al., 2000; Sutherland et al., 2012), because when subpopulations simultaneously encounter low abundance conditions, the ability of subpopulation with high abundance to compensate low abundance will be limited. On the other hand, the "portfolio effect" can be dampened as synchrony increases, reducing the resilience of population when facing stochastic environmental

doi:10.6342/NTU202301753

events or other perturbations (Schindler et al., 2010; Sullaway et al., 2021; Vargas et al., 2022). Consequently, asynchronous abundance fluctuations are the key to maintain the stability of population dynamics and ecosystem functionings; this pattern arises from heterogeneous environmental conditions, and proper harvesting strategies. My results demonstrate the detrimental effects of climate-promoted homogeneous environments and selective harvesting strategies on spatial synchrony, thereby increasing extinction risk of species (Figure S11). Ultimately, there is a pressing need of prevention and amendment for strong spatial synchrony, to reach the goal of persistence and sustainment of population dynamics.

doi:10.6342/NTU202301753

doi:10.6342/NTU202301753

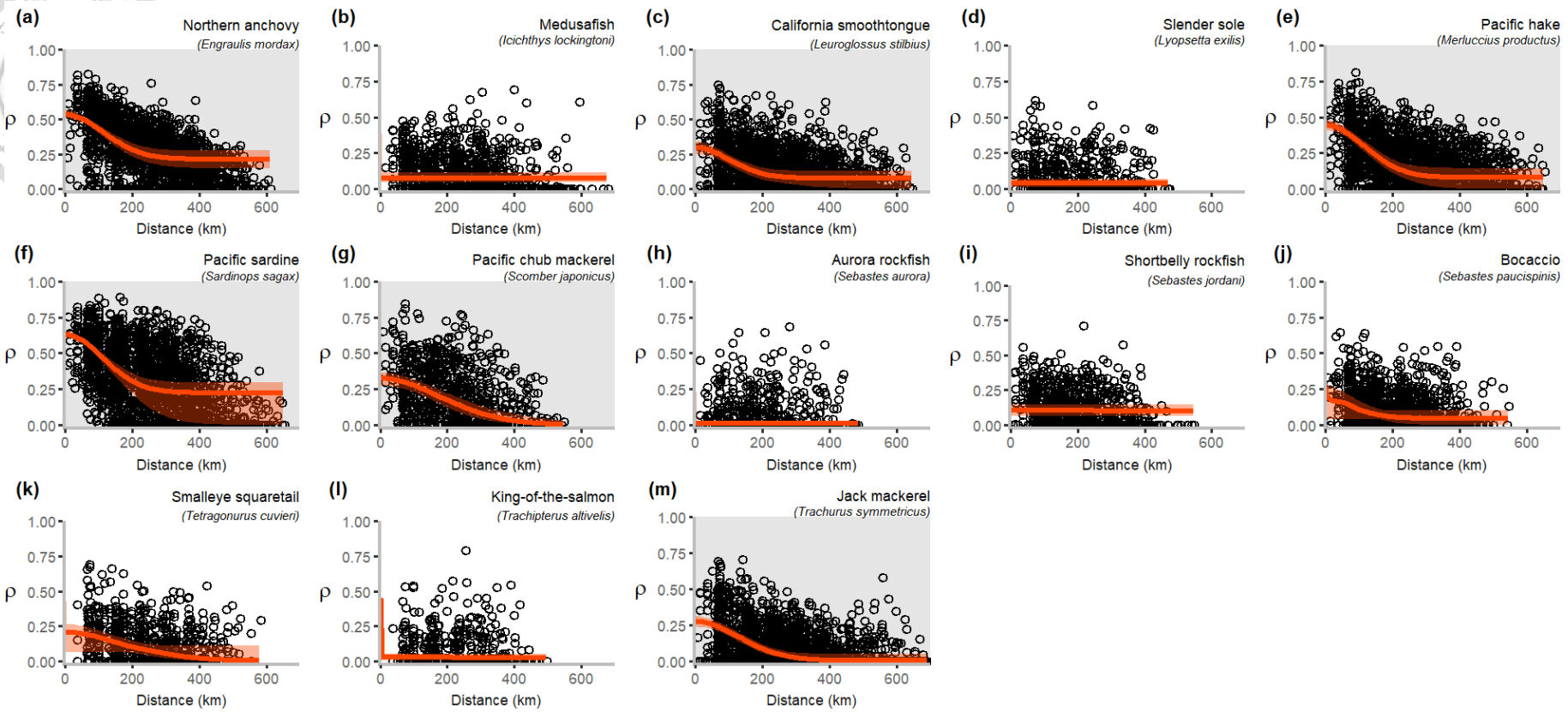

Figure 1. Spatial synchrony of fishes with occurrence stations > 30, y-axis is synchrony (ρ), x-axis is separate distance, and smoothers represent the 95% confidence intervals obtained from the bootstrapping estimation. Black points in behind are the station-pair correlations. Panels with grey backgrounds are the species with complete synchrony decay patterns.

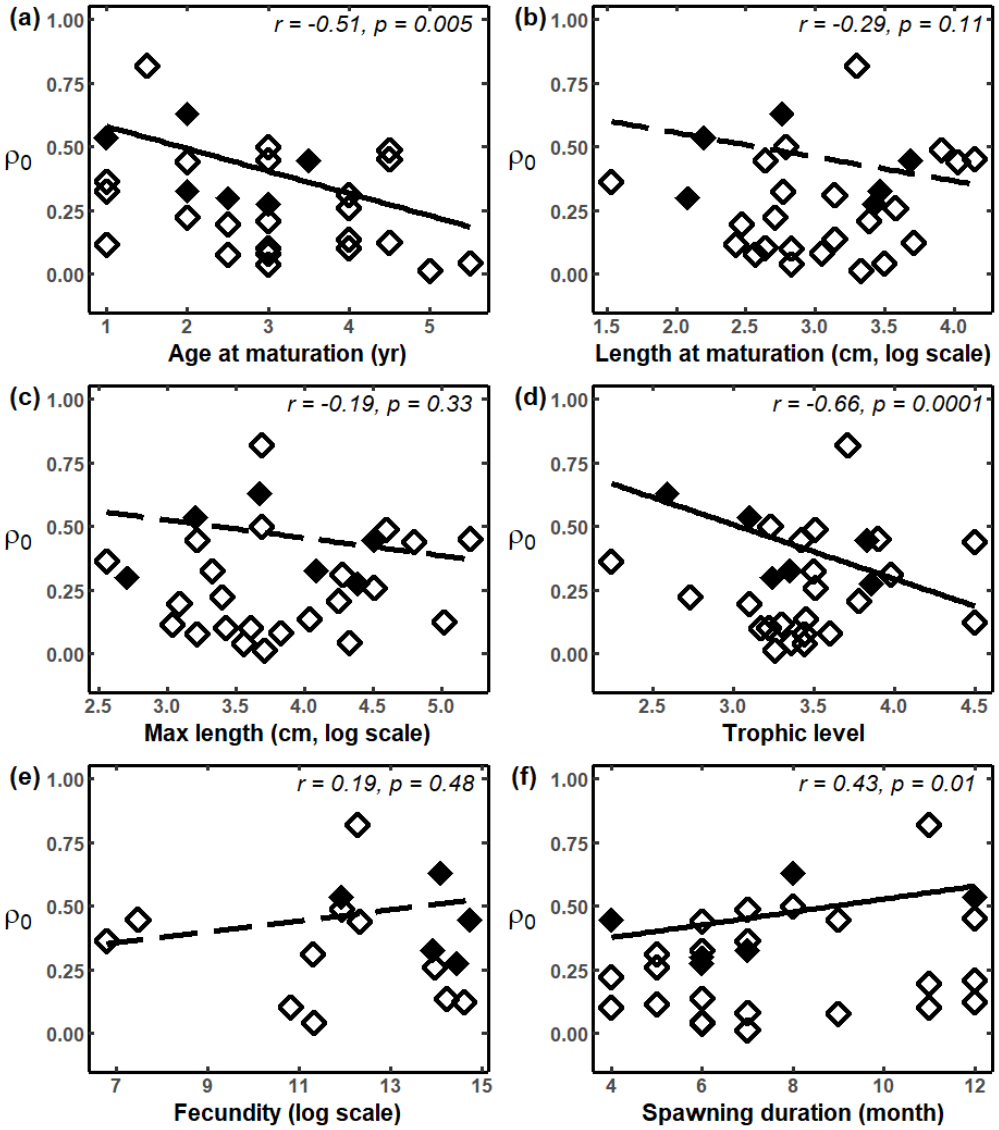

Figure 2. Spatial synchrony of distance approaching zero (ρ_0) versus life-history traits; each diamond represents a species, and solid diamonds represent species with complete synchrony decay pattern (6 species). Weighted least square regression is applied to describe the relationship between the two variables; weighted correlation coefficient and p-value for each trait is showed in the upper-right corner. The solid line indicates a significant regression, whereas the dotted line indicates a non-significant regression.

doi:10.6342/NTU202301753

doi:10.6342/NTU202301753

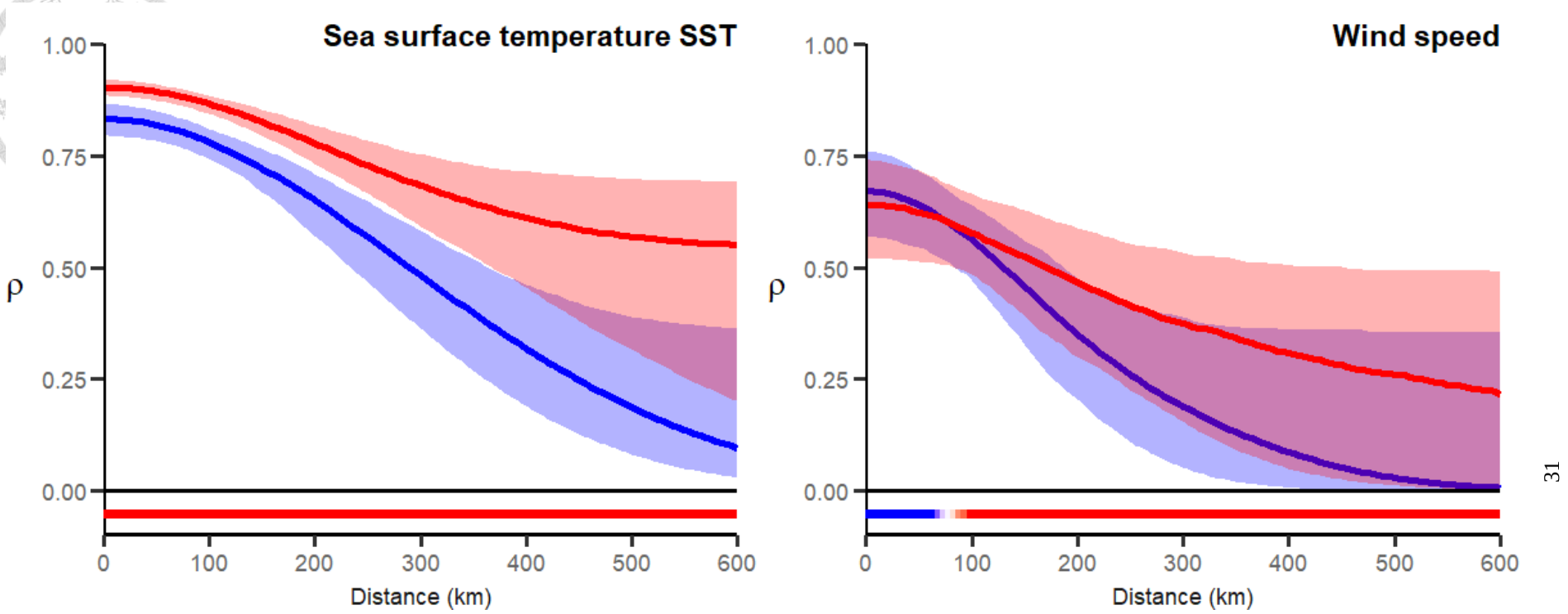

Figure 3. Spatial synchrony of environmental variables during climate transitions. The cold climate period is represented by blue line, and the warm climate period represented by red line. Smoothers represent the 95% confidence intervals that obtained from bootstrapping estimations. The color bar in the below is the difference between the two periods, indicating which period has higher synchrony at that distance range.

doi:10.6342/NTU202301753

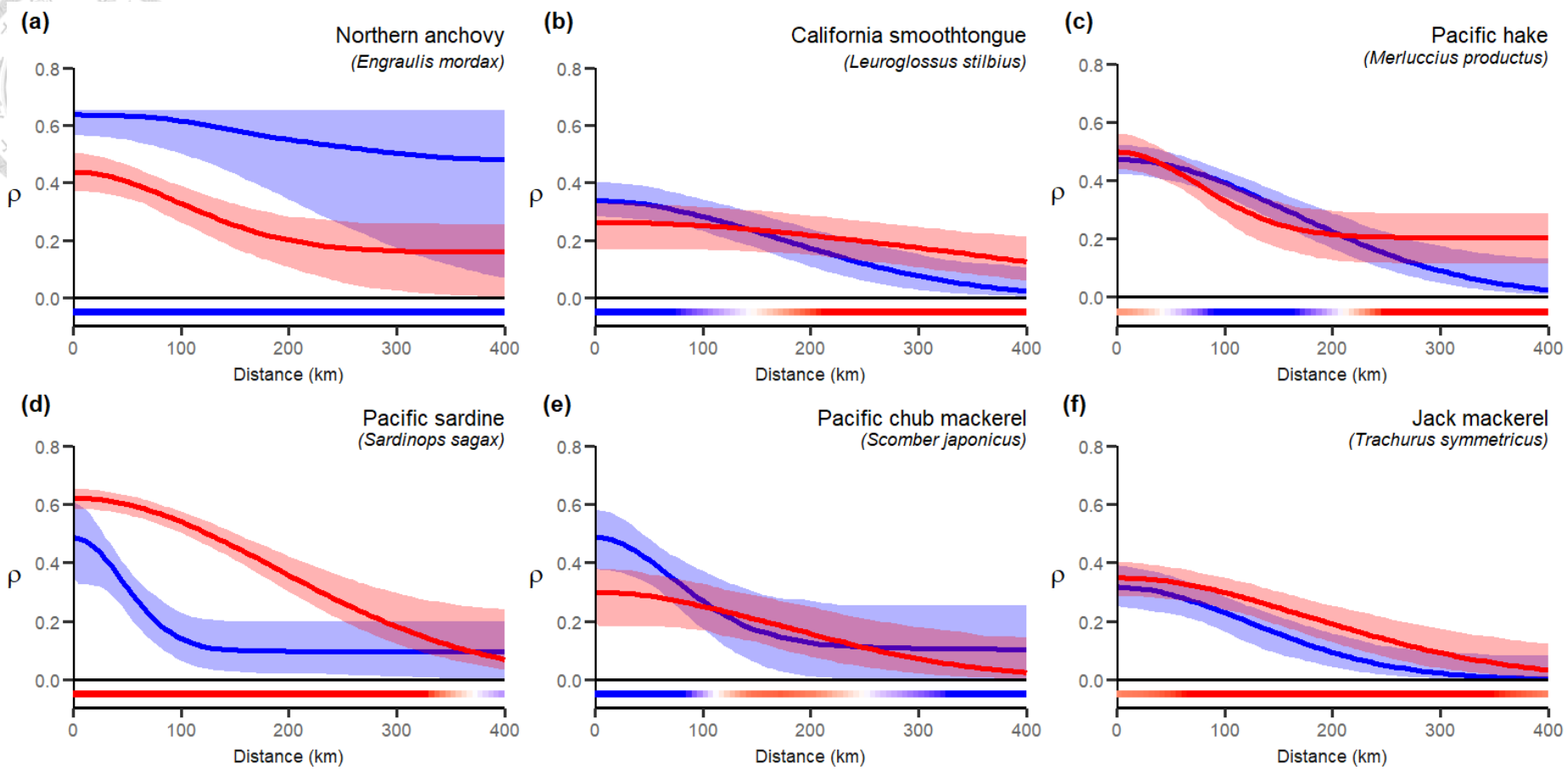

Figure 4. Spatial synchrony of fishes during climate transitions (with complete synchrony decay pattern). The cold climate period represented by blue line, and the warm climate period represented by red line. Smoothers represent the 95% confidence intervals that obtained from bootstrapping estimations. The color bar in the below is the difference between the two periods, indicating which period has higher synchrony at that distance range.

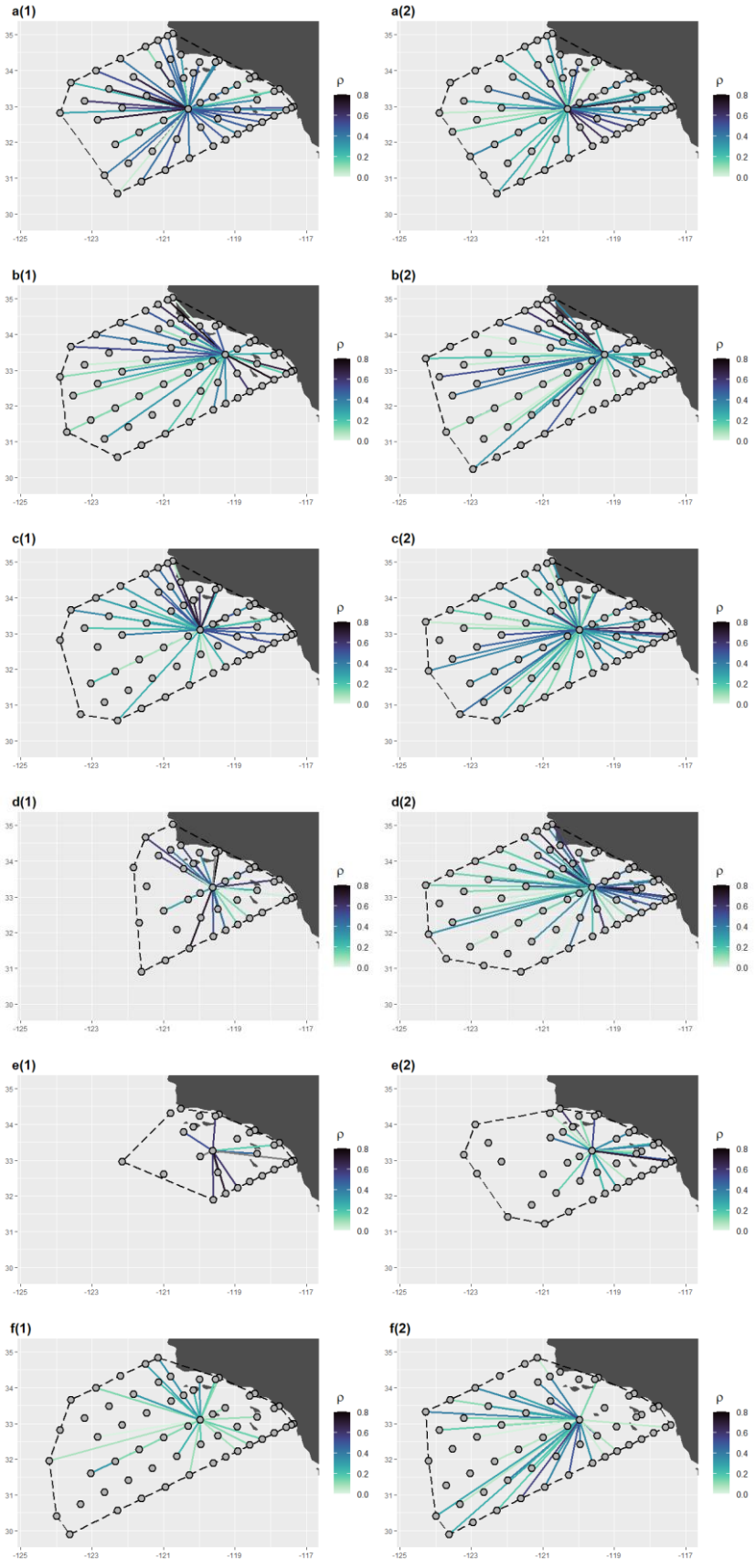

doi:10.6342/NTU202301753

Figure 5. Spatial-specific synchrony pattern during climate transitions, for (a) Northern anchovy, (b) California smoothtongue, (c) Pacific hake, (d) Pacific sardine, (e) Pacific chub mackerel, and (f) Jack mackerel in the (1) cold climate period and (2) warm climate period; the colored line represents the station-pair synchrony value (ρ).

doi:10.6342/NTU202301753

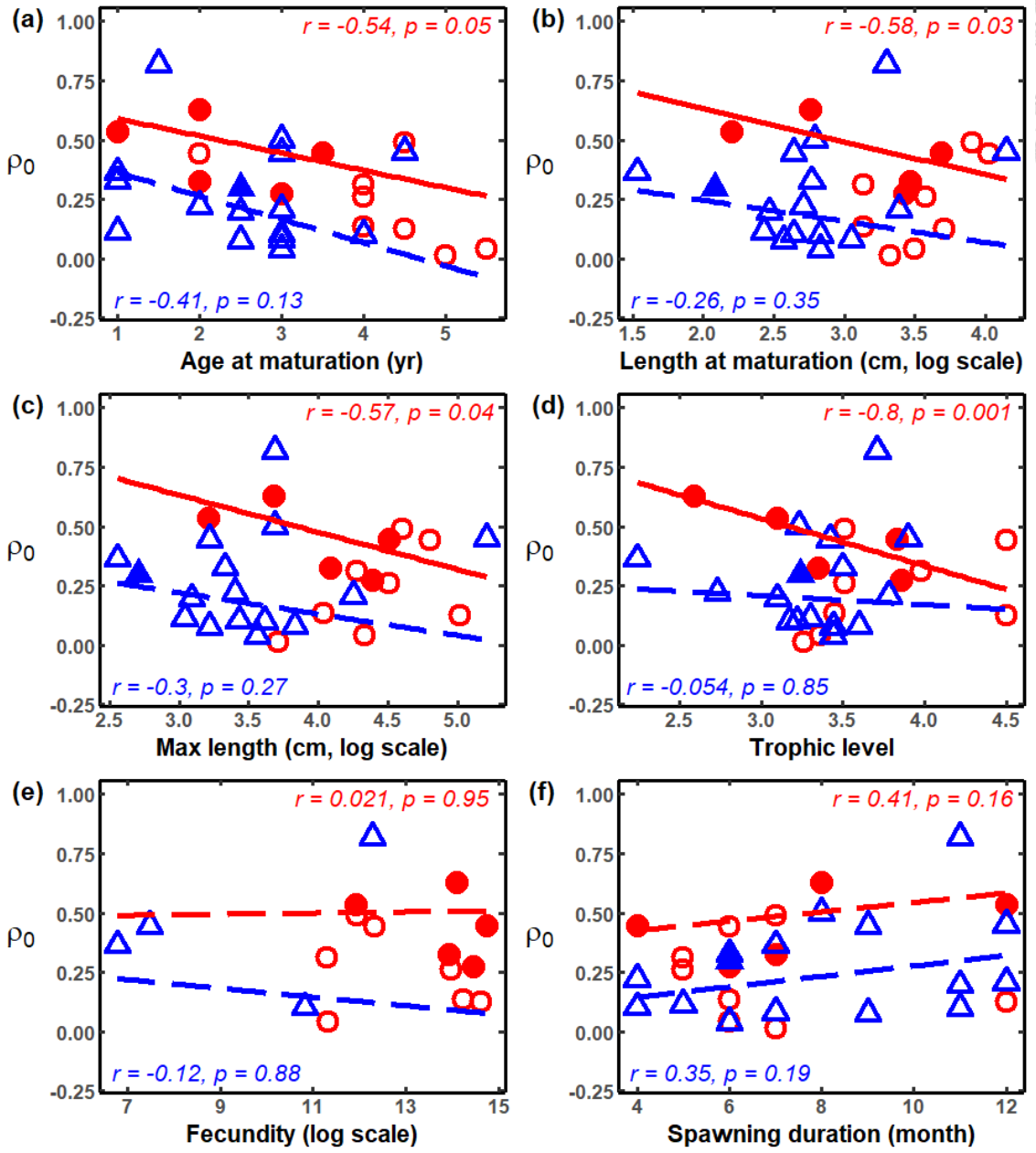

Figure 6. Spatial synchrony at distance approaching zero (ρ_0) of the exploited and unexploited species. Red circles represent exploited species; blue triangles represent unexploited species; solid form represents complete synchrony decay pattern; hollow form represents incomplete synchrony decay pattern. Weighted least square was applied to describe the relationship between the two variables; weighted correlation coefficient and p-value for each trait is showed in the corner.

doi:10.6342/NTU202301753

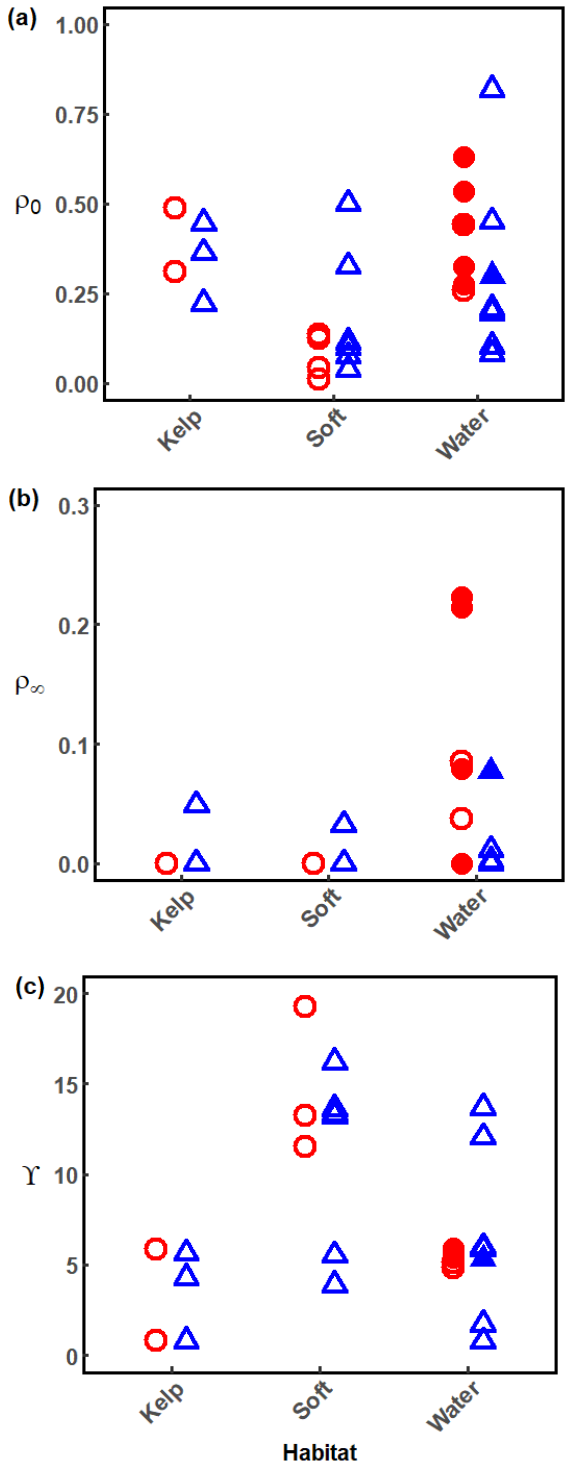

Figure 7. Spatial synchrony parameters versus habitat. Red circles represent exploited species; blue triangles represent unexploited species; solid from represents complete synchrony decay pattern (6 species).

doi:10.6342/NTU202301753

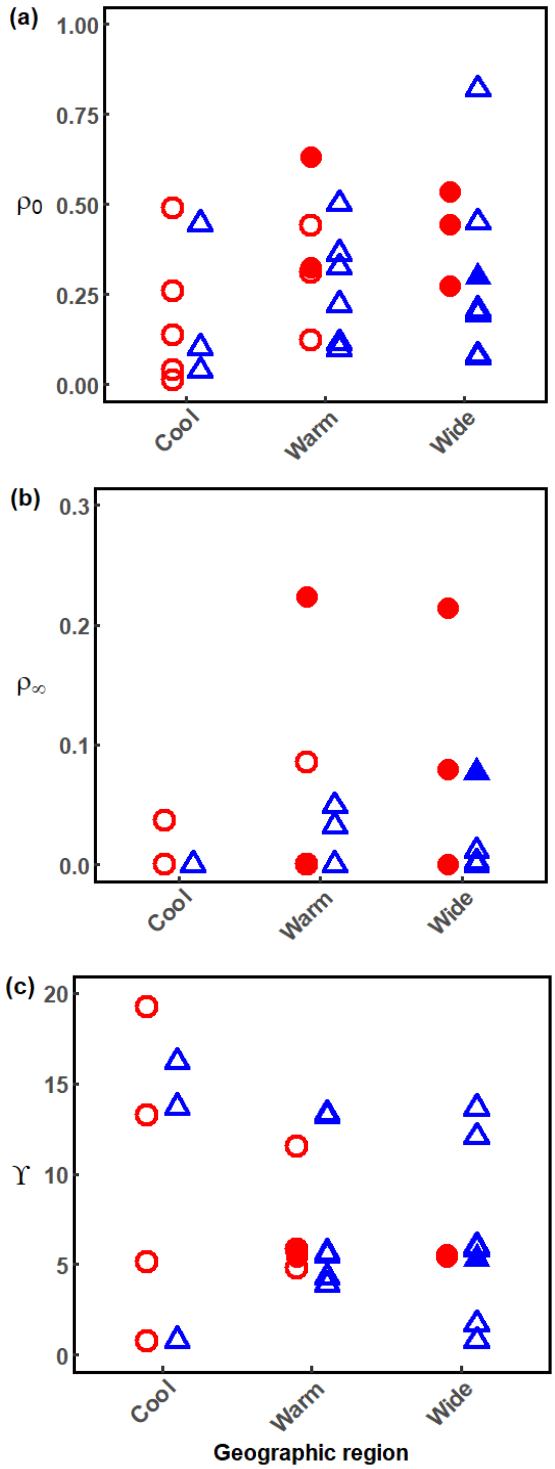

Figure 8. Spatial synchrony parameters versus geographic region. Red circles represent exploited species; blue triangles represent unexploited species; solid from represents complete synchrony decay pattern (6 species).

doi:10.6342/NTU202301753

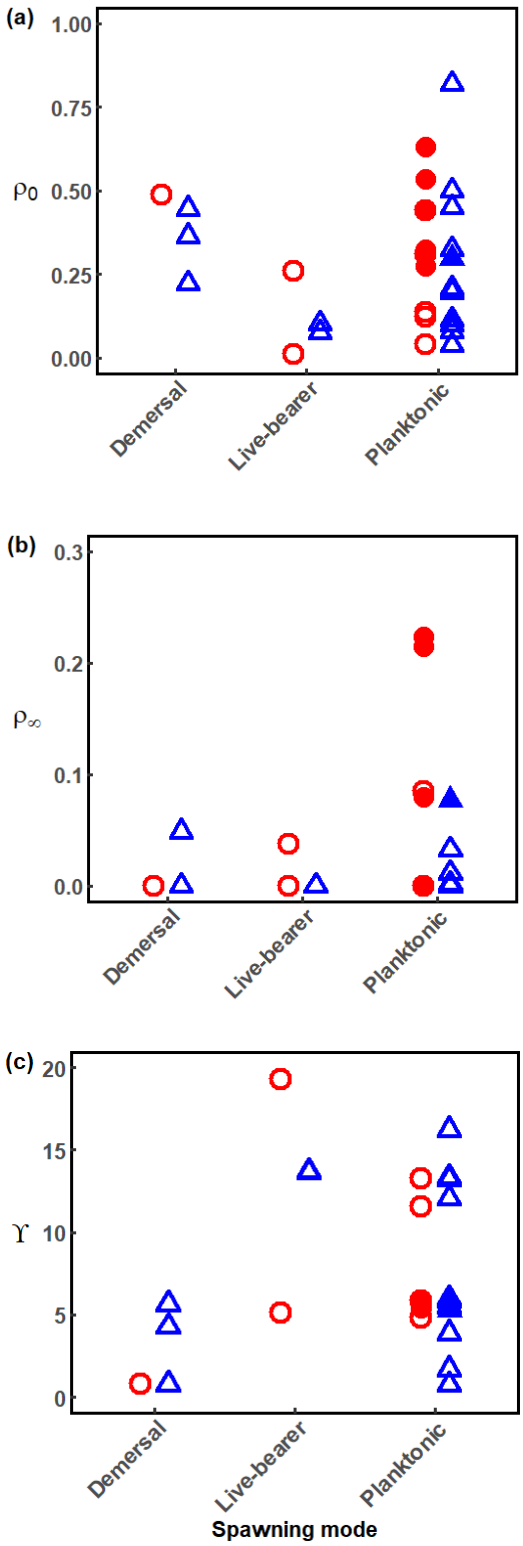

Figure 9. Spatial synchrony parameters versus spawning mode. Red circles represent exploited species; blue triangles represent unexploited species; solid from represents complete synchrony decay pattern (6 species).

doi:10.6342/NTU202301753

Table 1. Spatial synchrony at distance approaching zero ρ_0 estimation; * represents species with complete synchrony decay patterns.

Species	Common name	ρ_0	95% CI	
			Lower bound	Upper bound
Engraulis mordax	Northern anchovy	0.5349*	0.5070*	0.5654*
Merluccius productus	Pacific hake	0.4447*	0.4073*	0.4798*
Microstomus pacificus	Dover sole	0.0414	0.0056	0.6277
Paralabrax clathratus	Kelp bass	0.3108	0.2415	0.3807
Paralichthys californicus	California halibut	0.1237	0.0443	0.7467
Parophrys vetulus	English sole	0.1358	0.0687	0.2124
Sardinops sagax	Pacific sardine	0.6301*	0.6060*	0.6541*
Scomber japonicus	Pacific chub mackerel	0.3241*	0.2747*	0.3671*
Scorpaenichthys marmoratus	Cabezon	0.4881	0.0000	0.9985
Sebastes aurora	Aurora rockfish	0.0113	0.0000	0.4306
Sebastes paucispinis	Bocaccio	0.2593	0.0782	0.8550
Sphyraena argentea	Pacific barracuda	0.4406	0.2615	0.5891
Trachurus symmetricus	Jack mackerel	0.2748*	0.2382*	0.3165*
Argentina sialis	Pacific argentine	0.1959	0.0830	0.5962
Chromis punctipinnis	Blacksmith	0.2219	0.0970	0.6991
Cololabis saira	Pacific saury	0.8190	0.0004	0.9998
Hippoglossina stomata	Bigmouth sole	0.5008	0.1450	0.7160
Hypsoblennius jenkinsi	Mussel blenny	0.3638	0.0830	0.8975
Icichthys lockingtoni	Medusafish	0.0813	0.0451	0.6518
Leuroglossus stilbius	California smoothtongue	0.2980*	0.2529*	0.3460*
Lyopsetta exilis	Slender sole	0.0386	0.0136	0.0798
Ophidion scrippsae	Basketweave cusk-eel	0.3253	0.1734	0.7231
Oxylebius pictus	Painted greenling	0.4464	0.0000	0.9423
Pleuronichthys verticalis	Hornyhead turbot	0.1000	0.0327	0.7480
Sebastes jordani	Shortbelly rockfish	0.1030	0.0648	0.1501
Symphurus atricaudus	California tonguefish	0.1148	0.0528	0.6801
Tetragonurus cuvieri	Smalleye squaretail	0.2073	0.0680	0.5903
Trachipterus altivelis	King-of-the-salmon	0.4503	0.0072	0.6285
Zaniolepis frenata	Shortspine combfish	0.0757	0.0229	0.6991

doi:10.6342/NTU202301753

Table 2. Spatial synchrony at distance approaching infinite ρ_∞ estimation; * represents species with complete synchrony decay patterns.

Species	Common name	ρ_∞	95% CI	
			Lower bound	Upper bound
Engraulis mordax	Northern anchovy	0.2144*	0.1493*	0.2764*
Merluccius productus	Pacific hake	0.0793*	0.0000*	0.1448*
Microstomus pacificus	Dover sole	0.0000	0.0000	0.0434
Paralabrax clathratus	Kelp bass	0.0000	0.0000	0.0000
Paralichthys californicus	California halibut	0.0000	0.0000	0.1269
Parophrys vetulus	English sole	0.0000	0.0000	0.0000
Sardinops sagax	Pacific sardine	0.2233*	0.0000*	0.2948*
Scomber japonicus	Pacific chub mackerel	0.0000*	0.0000*	0.0000*
Scorpaenichthys marmoratus	Cabezon	0.0000	0.0000	0.0578
Sebastes aurora	Aurora rockfish	0.0000	0.0000	0.0094
Sebastes paucispinis	Bocaccio	0.0373	0.0000	0.0966
Sphyraena argentea	Pacific barracuda	0.0854	0.0000	0.2312
Trachurus symmetricus	Jack mackerel	0.0000*	0.0000*	0.0486*
Argentina sialis	Pacific argentine	0.0000	0.0000	0.0891
Chromis punctipinnis	Blacksmith	0.0000	0.0000	0.1089
Cololabis saira	Pacific saury	0.0020	0.0000	0.0247
Hippoglossina stomata	Bigmouth sole	0.0325	0.0000	0.1011
Hypsoblennius jenkinsi	Mussel blenny	0.0489	0.0000	0.1222
Icichthys lockingtoni	Medusafish	0.0000	0.0000	0.0809
Leuroglossus stilbius	California smoothtongue	0.0771*	0.0000*	0.1277*
Lyopsetta exilis	Slender sole	0.0000	0.0000	0.0000
Ophidion scrippsae	Basketweave cusk-eel	0.0000	0.0000	0.1251
Oxylebius pictus	Painted greenling	0.0000	0.0000	0.0571
Pleuronichthys verticalis	Hornyhead turbot	0.0000	0.0000	0.0870
Sebastes jordani	Shortbelly rockfish	0.0000	0.0000	0.0000
Symphurus atricaudus	California tonguefish	0.0000	0.0000	0.0987
Tetragonurus cuvieri	Smalleye squaretail	0.0000	0.0000	0.0652
Trachipterus altivelis	King-of-the-salmon	0.0113	0.0000	0.0417
Zaniolepis frenata	Shortspine combfish	0.0000	0.0000	0.0787

doi:10.6342/NTU202301753

Table 3. Spatial scaling l spatial synchrony estimation; * represents species with complete synchrony decay patterns.

			95% CI	
Species	Common name	Scale (km)	Lower bound	Upper bound
Engraulis mordax	Northern anchovy	114.09*	100.40*	131.81*
Merluccius productus	Pacific hake	115.12*	100.11*	133.41*
Microstomus pacificus	Dover sole	282601.37	1.02	15176393441.01
Paralabrax clathratus	Kelp bass	170.65	119.30	282.77
Paralichthys californicus	California halibut	51623.92	0.97	222010964.60
Parophrys vetulus	English sole	281385.35	405.81	790000384.08
Sardinops sagax	Pacific sardine	112.47*	101.45*	131.84*
Scomber japonicus	Pacific chub mackerel	181.19*	142.85*	228.70*
Scorpaenichthys marmoratus	Cabezon	1.09	0.01	635635384906769.00
Sebastes aurora	Aurora rockfish	117477236.93	1.13	51632538602452500.00
Sebastes paucispinis	Bocaccio	83.24	0.93	2513076.73
Sphyraena argentea	Pacific barracuda	60.51	15.33	368.54
Trachurus symmetricus	Jack mackerel	129.17*	106.96*	152.62*
Argentina sialis	Pacific argentine	198.79	1.23	5716392.00
Chromis punctipinnis	Blacksmith	141.57	1.02	1054112.67
Cololabis saira	Pacific saury	2.77	0.01	27.39
Hippoglossina stomata	Bigmouth sole	24.66	0.96	4109.62
Hypsoblennius jenkinsi	Mussel blenny	36.58	0.40	583493.13
Icichthys lockingtoni	Medusafish	85704.55	1.06	1295820325.29
Leuroglossus stilbius	California smoothtongue	101.90*	81.77*	132.35*
Lyopsetta exilis	Slender sole	5473997.43	460.74	21157994928.08
Ophidion scrippsae	Basketweave cusk-eel	125.41	6.90	19429.03
Oxylebius pictus	Painted greenling	1.11	0.96	2703034477650720.00
Pleuronichthys verticalis	Hornyhead turbot	310035.79	0.95	201302052.37
Sebastes jordani	Shortbelly rockfish	444543.36	708.62	4471740852.82
Symphurus atricaudus	California tonguefish	274757.97	1.00	148662550.87
Tetragonurus cuvieri	Smalleye squaretail	177.81	1.03	1069555.77
Trachipterus altivelis	King-of-the-salmon	1.07	0.99	29125389.25
Zaniolepis frenata	Shortspine combfish	419955.50	1.00	867866563.33

doi:10.6342/NTU202301753

Table 4. Decay function γ estimation; * represents species with complete synchrony decay patterns.

Species	Common name	γ	95% CI	
			Lower bound	Upper bound
Engraulis mordax	Northern anchovy	5.43*	5.30*	5.57*
Merluccius productus	Pacific hake	5.44*	5.30*	5.59*
Microstomus pacificus	Dover sole	13.24	0.71	24.14
Paralabrax clathratus	Kelp bass	5.83	5.47	6.34
Paralichthys californicus	California halibut	11.54	0.66	19.91
Parophrys vetulus	English sole	13.24	6.70	21.18
Sardinops sagax	Pacific sardine	5.42*	5.31*	5.57*
Scomber japonicus	Pacific chub mackerel	5.89*	5.65*	6.13*
Scorpaenichthys marmoratus	Cabezon	0.78	-3.76	34.78
Sebastes aurora	Aurora rockfish	19.27	0.82	39.18
Sebastes paucispinis	Bocaccio	5.11	0.63	15.43
Sphyraena argentea	Pacific barracuda	4.80	3.42	6.60
Trachurus symmetricus	Jack mackerel	5.55*	5.37*	5.72*
Argentina sialis	Pacific argentine	5.99	0.90	16.25
Chromis punctipinnis	Blacksmith	5.65	0.71	14.56
Cololabis saira	Pacific saury	1.71	-3.62	4.00
Hippoglossina stomata	Bigmouth sole	3.90	0.65	9.01
Hypsoblennius jenkinsi	Mussel blenny	4.29	-0.23	13.97
Icichthys lockingtoni	Medusafish	12.05	0.75	21.68
Leuroglossus stilbius	California smoothtongue	5.32*	5.10*	5.58*
Lyopsetta exilis	Slender sole	16.21	6.83	24.47
Ophidion scrippsae	Basketweave cusk-eel	5.52	2.62	10.57
Oxylebius pictus	Painted greenling	0.80	0.66	36.23
Pleuronichthys verticalis	Hornyhead turbot	13.34	0.65	19.81
Sebastes jordani	Shortbelly rockfish	13.70	7.26	22.91
Symphurus atricaudus	California tonguefish	13.22	0.69	19.51
Tetragonurus cuvieri	Smalleye squaretail	5.87	0.73	14.58
Trachipterus altivelis	King-of-the-salmon	0.76	0.69	17.88
Zaniolepis frenata	Shortspine combfish	13.64	0.69	21.27

doi:10.6342/NTU202301753

References

Adams, C. F., Alade, L. A., Legault, C. M., O'Brien, L., Palmer, M. C., Sosebee, K. A., & Traver, M. L. (2018). Relative importance of population size, fishing pressure and temperature on the spatial distribution of nine Northwest Atlantic groundfish stocks. *PLoS One*, *13*(4), e0196583.

Bell, R. J., Richardson, D. E., Hare, J. A., Lynch, P. D., & Fratantoni, P. S. (2015). Disentangling the effects of climate, abundance, and size on the distribution of marine fish: an example based on four stocks from the Northeast US shelf. *ICES Journal of Marine Science*, *72*(5), 1311-1322.

Berkeley, S. A., Hixon, M. A., Larson, R. J., & Love, M. S. (2004). Fisheries sustainability via protection of age structure and spatial distribution of fish populations. *Fisheries*, *29*(8), 23-32.

BjØrnstad, O. N., & Falck, W. (2001). Nonparametric spatial covariance functions: estimation and testing. *Environmental and Ecological Statistics*, *8*, 53-70.

Brown, J. H., & Kodric-Brown, A. (1977). Turnover rates in insular biogeography: effect of immigration on extinction. *Ecology*, *58*(2), 445-449.

Buelga Díaz, A., Castañón Fernández, C., Ares, G., Prieto, D. A., & Álvarez, I. D. (2022). RecMin Variograms: visualisation and three-dimensional calculation of variograms in block modelling applications in Geology and Mining. *International*

doi:10.6342/NTU202301753

Journal of Environmental Research and Public Health, *19*(19), 12454.

Cressie, N., & Wikle, C. K. (2015). *Statistics for spatio-temporal data*. John Wiley & Sons.

Defriez, E. J., Sheppard, L. W., Reid, P. C., & Reuman, D. C. (2016). Climate change-related regime shifts have altered spatial synchrony of plankton dynamics in the North Sea. *Global change biology*, *22*(6), 2069-2080.

Di Cecco, G. J., & Gouhier, T. C. (2018). Increased spatial and temporal autocorrelation of temperature under climate change. *Sci Rep*, *8*(1), 14850. https://doi.org/10.1038/s41598-018-33217-0

Earn, D. J., Levin, S. A., & Rohani, P. (2000). Coherence and conservation. *Science*, *290*(5495), 1360-1364.

Engelhard, G. H., Righton, D. A., & Pinnegar, J. K. (2014). Climate change and fishing: a century of shifting distribution in North Sea cod. *Global change biology*, *20*(8), 2473-2483.

Engen, S., Lande, R., & Sæther, B.-E. (2002). The spatial scale of population fluctuations and quasi-extinction risk. *The American Naturalist*, *160*(4), 439-451.

Engen, S., Lande, R., Sæther, B.-E., & Bregnballe, T. (2005). Estimating the pattern of synchrony in fluctuating populations. *Journal of Animal Ecology*, 601-611.

Engen, S., Lee, A. M., & Sæther, B.-E. (2018). Spatial distribution and optimal harvesting

doi:10.6342/NTU202301753

of an age-structured population in a fluctuating environment. *Mathematical biosciences*, *296*, 36-44.

Frank, K. T., Petrie, B., Leggett, W. C., & Boyce, D. G. (2016). Large scale, synchronous variability of marine fish populations driven by commercial exploitation. *Proceedings of the National Academy of Sciences of USA*, *113*(29), 8248-8253.

Garcia, S. M., Kolding, J., Rice, J., Rochet, M.-J., Zhou, S., Arimoto, T., Beyer, J., Borges, L., Bundy, A., & Dunn, D. (2012). Reconsidering the consequences of selective fisheries. *science*, *335*(6072), 1045-1047.

Grøtan, V., Sæther, B.-E., Engen, S., Solberg, E. J., Linnell, J. D., Andersen, R., Brøseth, H., & Lund, E. (2005). Climate causes large-scale spatial synchrony in population fluctuations of a temperate herbivore. *Ecology*, *86*(6), 1472-1482.

Hixon, M. A., Johnson, D. W., & Sogard, S. M. (2014). BOFFFFs: on the importance of conserving old-growth age structure in fishery populations. *ICES Journal of Marine Science*, *71*(8), 2171-2185.

Hsieh, C.-h., Reiss, C., Watson, W., Allen, M. J., Hunter, J. R., Lea, R. N., Rosenblatt, R. H., Smith, P. E., & Sugihara, G. (2005). A comparison of long-term trends and variability in populations of larvae of exploited and unexploited fishes in the Southern California region: A community approach. *Progress in oceanography*, *67*(1-2), 160-185.

doi:10.6342/NTU202301753

Hsieh, C.-h., Reiss, C. S., Hewitt, R. P., & Sugihara, G. (2008). Spatial analysis shows that fishing enhances the climatic sensitivity of marine fishes. *Canadian Journal of Fisheries and Aquatic Sciences*, *65*(5), 947-961. https://doi.org/10.1139/f08-017

Hsieh, c. H., Kim, H. J., Watson, W., Di Lorenzo, E., & Sugihara, G. (2009). Climate-driven changes in abundance and distribution of larvae of oceanic fishes in the southern California region. *Global change biology*, *15*(9), 2137-2152.

Hsieh, C. H., Reiss, C. S., Hunter, J. R., Beddington, J. R., May, R. M., & Sugihara, G. (2006). Fishing elevates variability in the abundance of exploited species. *Nature*, *443*(7113), 859-862. https://doi.org/10.1038/nature05232

Huse, G., Fernö, A., & Holst, J. C. (2010). Establishment of new wintering areas in herring co-occurs with peaks in the 'first time/repeat spawner'ratio. *Marine Ecology Progress Series*, *409*, 189-198.

Jared, T., Daniel, L., Michael, L., Tyler, D., Thomas, R., Randall, M., Mark, P., & Eric, K. (2015). Spatial synchrony in cisco recruitment. *Fisheries research*.

Koenig, W. D., & Liebhold, A. M. (2016). Temporally increasing spatial synchrony of North American temperature and bird populations. *Nature Climate Change*, *6*(6), 614-617.

Krebs, C. J., Boonstra, R., Boutin, S., & Sinclair, A. R. (2001). What drives the 10-year

doi:10.6342/NTU202301753

cycle of snowshoe hares? The ten-year cycle of snowshoe hares—one of the most striking features of the boreal forest—is a product of the interaction between predation and food supplies, as large-scale experiments in the Yukon have demonstrated. *BioScience*, *51*(1), 25-35.

Kuo, T. C., Mandal, S., Yamauchi, A., & Hsieh, C. h. (2016). Life history traits and exploitation affect the spatial mean-variance relationship in fish abundance. *Ecology*, *97*(5), 1251-1259.

Lande, R., Engen, S., & Sæther, B.-E. (1999). Spatial scale of population synchrony: environmental correlation versus dispersal and density regulation. *The American Naturalist*, *154*(3), 271-281.

Liebhold, A., Koenig, W. D., & Bjørnstad, O. N. (2004). Spatial synchrony in population dynamics. *Annu. Rev. Ecol. Evol. Syst.*, *35*, 467-490.

Lindegren, M., & Checkley Jr, D. M. (2013). Temperature dependence of Pacific sardine (Sardinops sagax) recruitment in the California Current Ecosystem revisited and revised. *Canadian Journal of Fisheries and Aquatic Sciences*, *70*(2), 245-252.

Marquez, J. F., Lee, A. M., Aanes, S., Engen, S., Herfindal, I., Salthaug, A., & Saether, B. E. (2019). Spatial scaling of population synchrony in marine fish depends on their life history. *Ecol Lett*, *22*(11), 1787-1796. https://doi.org/10.1111/ele.13360

Marquez, J. F., Sæther, B. E., Aanes, S., Engen, S., Salthaug, A., & Lee, A. M. (2021).

doi:10.6342/NTU202301753

Age-dependent patterns of spatial autocorrelation in fish populations. *Ecology*, *102*(12), e03523.

Moran, P. A. (1953). The statistical analysis of the Canadian lynx cycle. *Australian Journal of Zoology*, *1*(3), 291-298.

Myers, R., Mertz, G., & Bridson, J. (1997). Spatial scales of interannual recruitment variations of marine, anadromous, and freshwater fish. *Canadian Journal of Fisheries and Aquatic Sciences*, *54*(6), 1400-1407.

Nicolau, P. G., Ims, R. A., Sorbye, S. H., & Yoccoz, N. G. (2022). Seasonality, density dependence, and spatial population synchrony. *Proc Natl Acad Sci U S A*, *119*(51), e2210144119. https://doi.org/10.1073/pnas.2210144119

Oken, K. L., Holland, D. S., & Punt, A. E. (2021). The effects of population synchrony, life history, and access constraints on benefits from fishing portfolios. *Ecological Applications*, *31*(4), e2307.

Pan, R. Y., Kuo, T. C., & Hsieh, C. h. (2021). Hump-shaped relationship between aggregation tendency and body size within fish populations. *Ecography*, *44*(9), 1418-1427.

Paradis, E., Baillie, S., Sutherland, W., & Gregory, R. (1999). Dispersal and spatial scale affect synchrony in spatial population dynamics. *Ecology Letters*, *2*(2), 114-120.

Paradis, E., Baillie, S. R., Sutherland, W. J., & Gregory, R. D. (2000). Spatial synchrony

doi:10.6342/NTU202301753

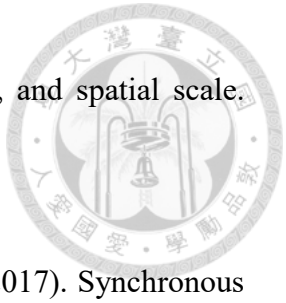

in populations of birds: effects of habitat, population trend, and spatial scale. *Ecology*, *81*(8), 2112-2125.

Pardikes, N. A., Harrison, J. G., Shapiro, A. M., & Forister, M. L. (2017). Synchronous population dynamics in California butterflies explained by climatic forcing. *Royal Society open science*, *4*(7), 170190.

Perry, A. L., Low, P. J., Ellis, J. R., & Reynolds, J. D. (2005). Climate change and distribution shifts in marine fishes. *Science*, *308*(5730), 1912-1915.

Petatán-Ramírez, D., Ojeda-Ruiz, M. Á., Sánchez-Velasco, L., Rivas, D., Reyes-Bonilla, H., Cruz-Piñón, G., Morzaria-Luna, H. N., Cisneros-Montemayor, A. M., Cheung, W., & Salvadeo, C. (2019). Potential changes in the distribution of suitable habitat for Pacific sardine (*Sardinops sagax*) under climate change scenarios. *Deep Sea Research Part II: Topical Studies in Oceanography*, *169*, 104632.

Planque, B., Fromentin, J.-M., Cury, P., Drinkwater, K. F., Jennings, S., Perry, R. I., & Kifani, S. (2010). How does fishing alter marine populations and ecosystems sensitivity to climate? *Journal of Marine Systems*, *79*(3-4), 403-417.

Post, E., & Forchhammer, M. C. (2002). Synchronization of animal population dynamics by large-scale climate. *Nature*, *420*(6912), 168-171.

Post, E., & Forchhammer, M. C. (2004). Spatial synchrony of local populations has increased in association with the recent Northern Hemisphere climate trend.

doi:10.6342/NTU202301753

Proceedings of the National Academy of Sciences of USA, *101*(25), 9286-9290.

Ranta, E., Kaitala, V., Lindström, J., & Linden, H. (1995). Synchrony in population dynamics. *Proceedings of the Royal Society of London. Series B: Biological Sciences*, *262*(1364), 113-118.

Sang, H., & Huang, J. Z. (2012). A full scale approximation of covariance functions for large spatial data sets. *Journal of the Royal Statistical Society Series B: Statistical Methodology*, *74*(1), 111-132.

Schindler, D. E., Hilborn, R., Chasco, B., Boatright, C. P., Quinn, T. P., Rogers, L. A., & Webster, M. S. (2010). Population diversity and the portfolio effect in an exploited species. *Nature*, *465*(7298), 609-612.

Sheppard, L. W., Bell, J. R., Harrington, R., & Reuman, D. C. (2016). Changes in large-scale climate alter spatial synchrony of aphid pests. *Nature Climate Change*, *6*(6), 610-613.

Sheppard, L. W., Defriez, E. J., Reid, P. C., & Reuman, D. C. (2019). Synchrony is more than its top-down and climatic parts: interacting Moran effects on phytoplankton in British seas. *PLoS Computational Biology*, *15*(3), e1006744.

Sherman, M. (2011). *Spatial statistics and spatio-temporal data: covariance functions and directional properties*. John Wiley & Sons.

Stowe, E. S., Wenger, S. J., Freeman, M. C., & Freeman, B. J. (2020). Incorporating

doi:10.6342/NTU202301753

spatial synchrony in the status assessment of a threatened species with multivariate analysis. *Biological Conservation*, *248*, 108612.

Stuart-Smith, R. D. (2021). Climate change: Large-scale abundance shifts in fishes. *Current Biology*, *31*(21), R1445-R1447.

Sullaway, G. H., Shelton, A. O., & Samhouri, J. F. (2021). Synchrony erodes spatial portfolios of an anadromous fish and alters availability for resource users. *Journal of Animal Ecology*, *90*(11), 2692-2703.

Sutherland, C., Elston, D. A., & Lambin, X. (2012). Multi-scale processes in metapopulations: contributions of stage structure, rescue effect, and correlated extinctions. *Ecology*, *93*(11), 2465-2473.

Vargas, A., Restrepo, S., & Diaz, D. (2022). The portfolio effect in a small-scale fishery reduces catch and fishing income variability in a highly dynamic ecosystem. *PLoS One*, *17*(8), e0271172.

Walter, J. A., Sheppard, L. W., Anderson, T. L., Kastens, J. H., Bjørnstad, O. N., Liebhold, A. M., & Reuman, D. C. (2017). The geography of spatial synchrony. *Ecology Letters*, *20*(7), 801-814.

Wang, D., Gouhier, T. C., Menge, B. A., & Ganguly, A. R. (2015). Intensification and spatial homogenization of coastal upwelling under climate change. *Nature*, *518*(7539), 390-394.

doi:10.6342/NTU202301753

Wang, H.-Y., Shen, S.-F., Chen, Y.-S., Kiang, Y.-K., & Heino, M. (2020). Life histories determine divergent population trends for fishes under climate warming. *Nature Communications*, *11*(1), 4088.

Wu, L., Cai, W., Zhang, L., Nakamura, H., Timmermann, A., Joyce, T., McPhaden, M. J., Alexander, M., Qiu, B., & Visbeck, M. (2012). Enhanced warming over the global subtropical western boundary currents. *Nature Climate Change*, *2*(3), 161-166.

Zhang, B., Sang, H., & Huang, J. Z. (2015). Full-scale approximations of spatio-temporal covariance models for large datasets. *Statistica Sinica*, 99-114.

doi:10.6342/NTU202301753

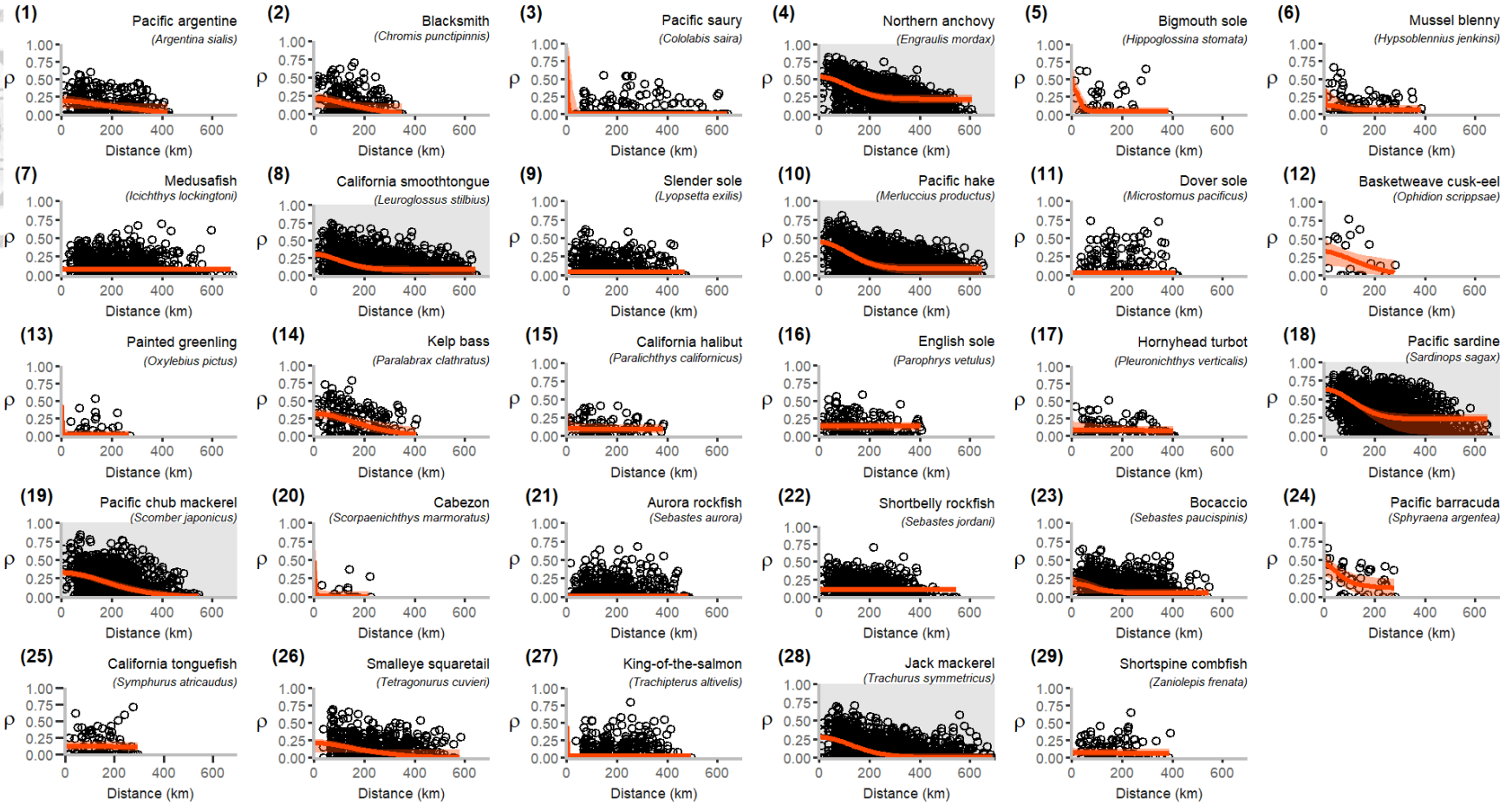

Appendix

Figure S1. Spatial synchrony of 29 fish species, y-axis is synchrony (ρ), x-axis is separate distance, and smoothers represent the 95% confidence intervals obtained from the bootstrapping estimation. Black points in behind are the station-pair correlations. Panels with grey backgrounds are the species with complete synchrony decay patterns.

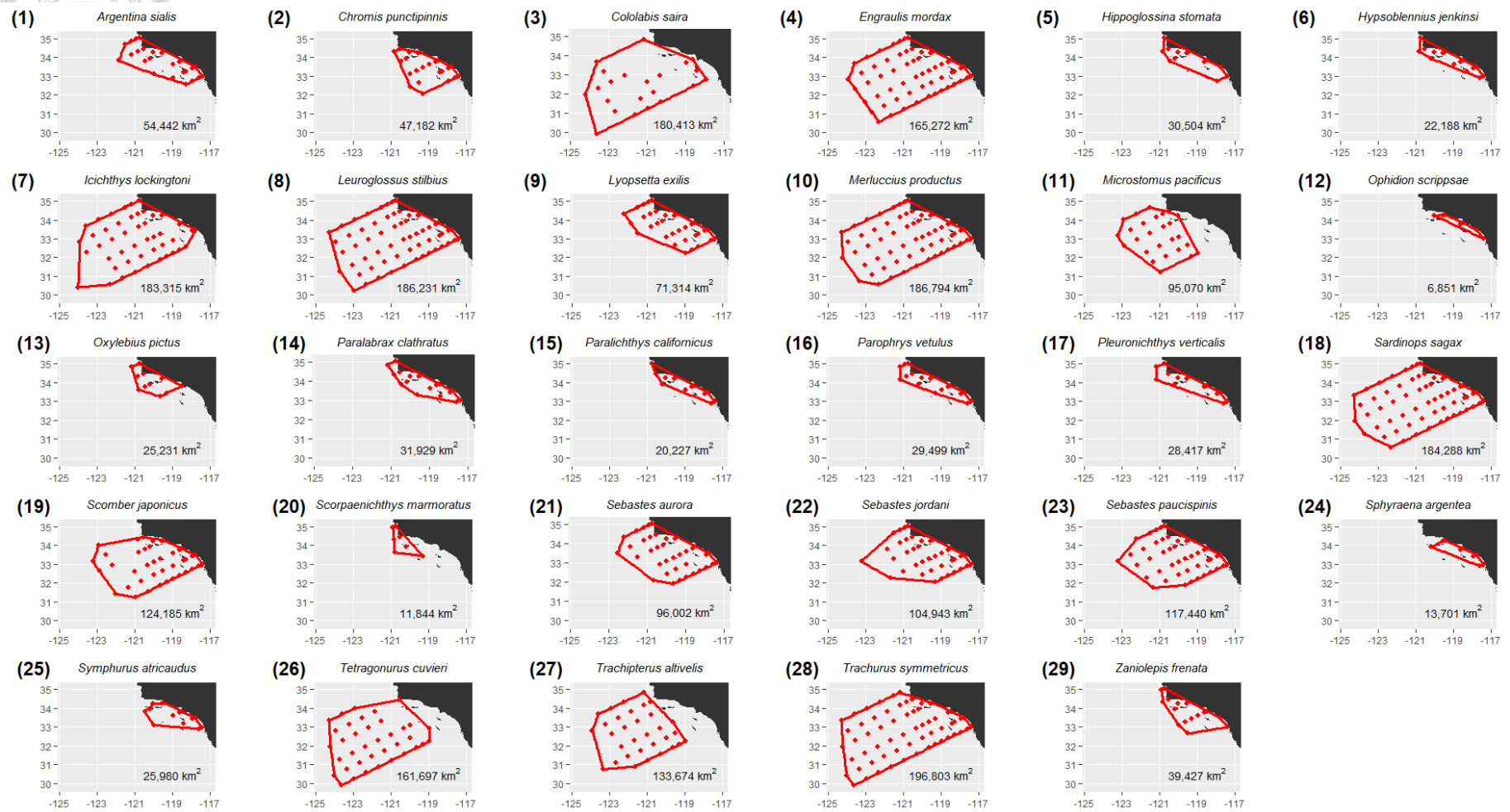

Figure S2. Principal spawning areas for all species. The red dots are the occurred stations, and polygon that encompass the occurred stations is the principal spawning area, measured by convex hull.

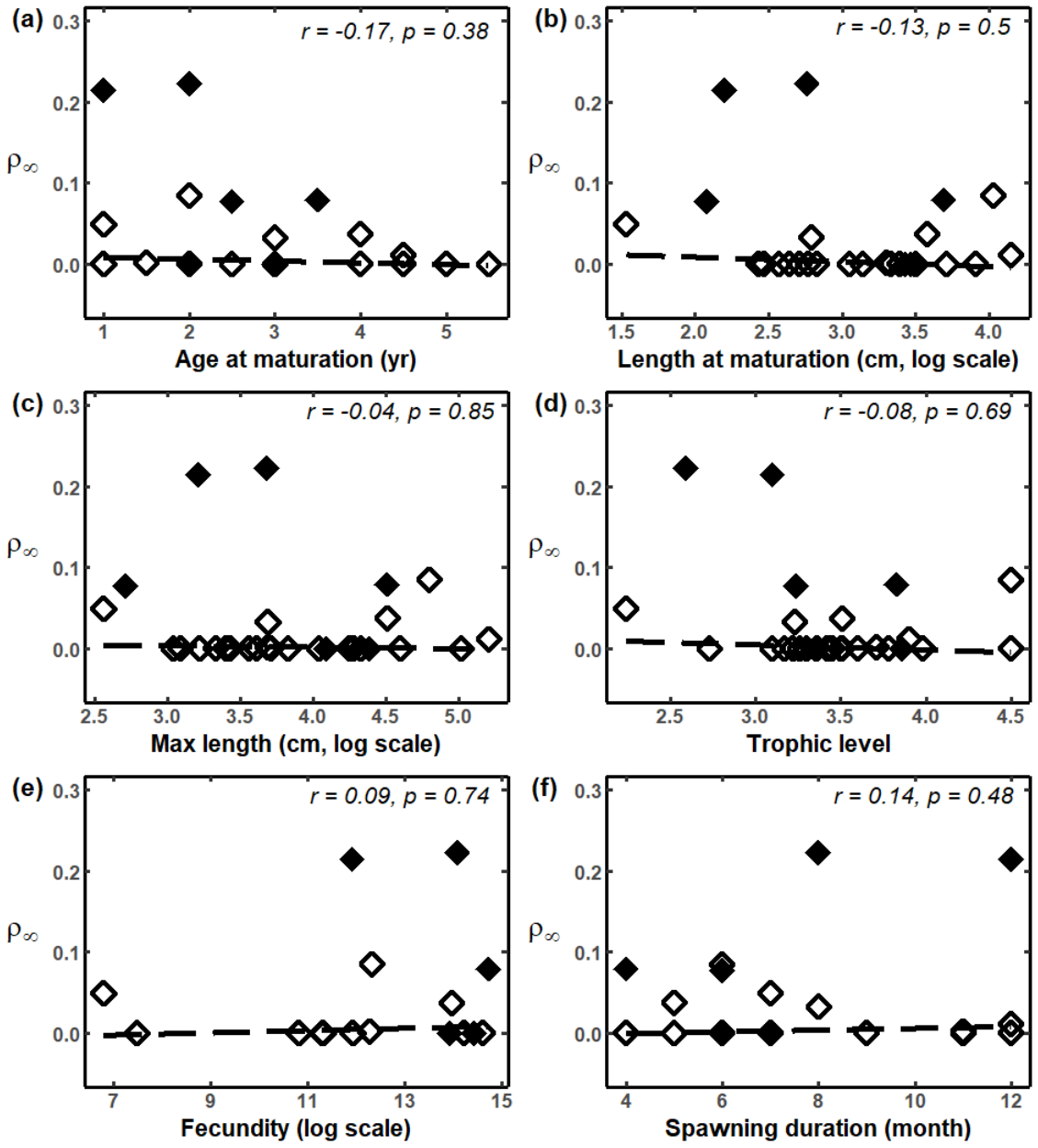

Figure S3. ρ_{∞} versus life-history traits; each diamond represents a species and solid diamonds represent species with complete synchrony decay pattern (6 species). Weighted least square regression is applied to describe the relationship between the two variables; weighted correlation coefficient and p-value for each trait is showed in the upper-right corner.

doi:10.6342/NTU202301753

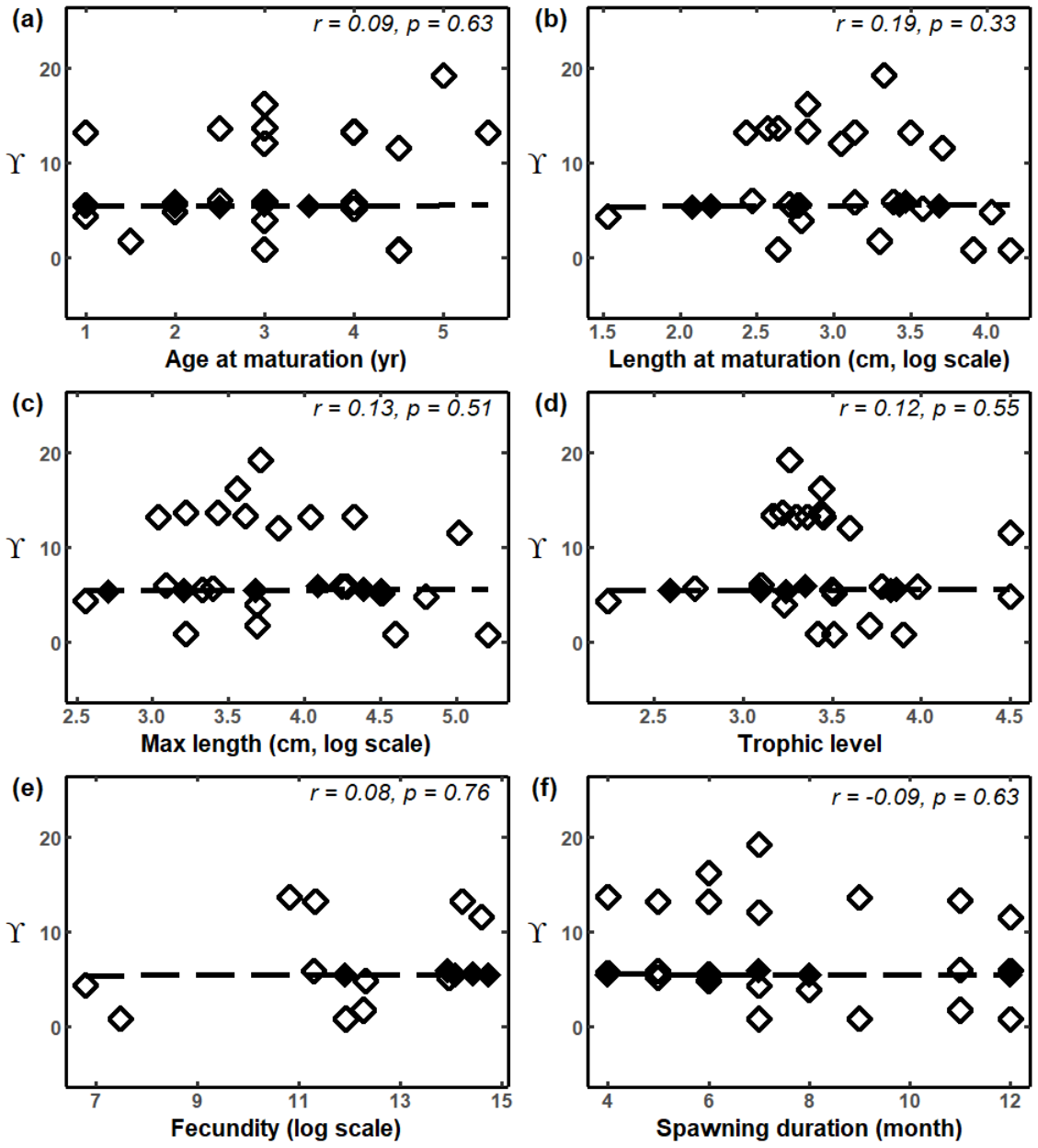

Figure S4. γ versus life-history traits; each diamond represents a species and solid diamonds represent species with complete synchrony decay pattern (6 species). Weighted least square regression is applied to describe the relationship between the two variables; weighted correlation coefficient and p-value for each trait is showed in the upper-right corner.

doi:10.6342/NTU202301753

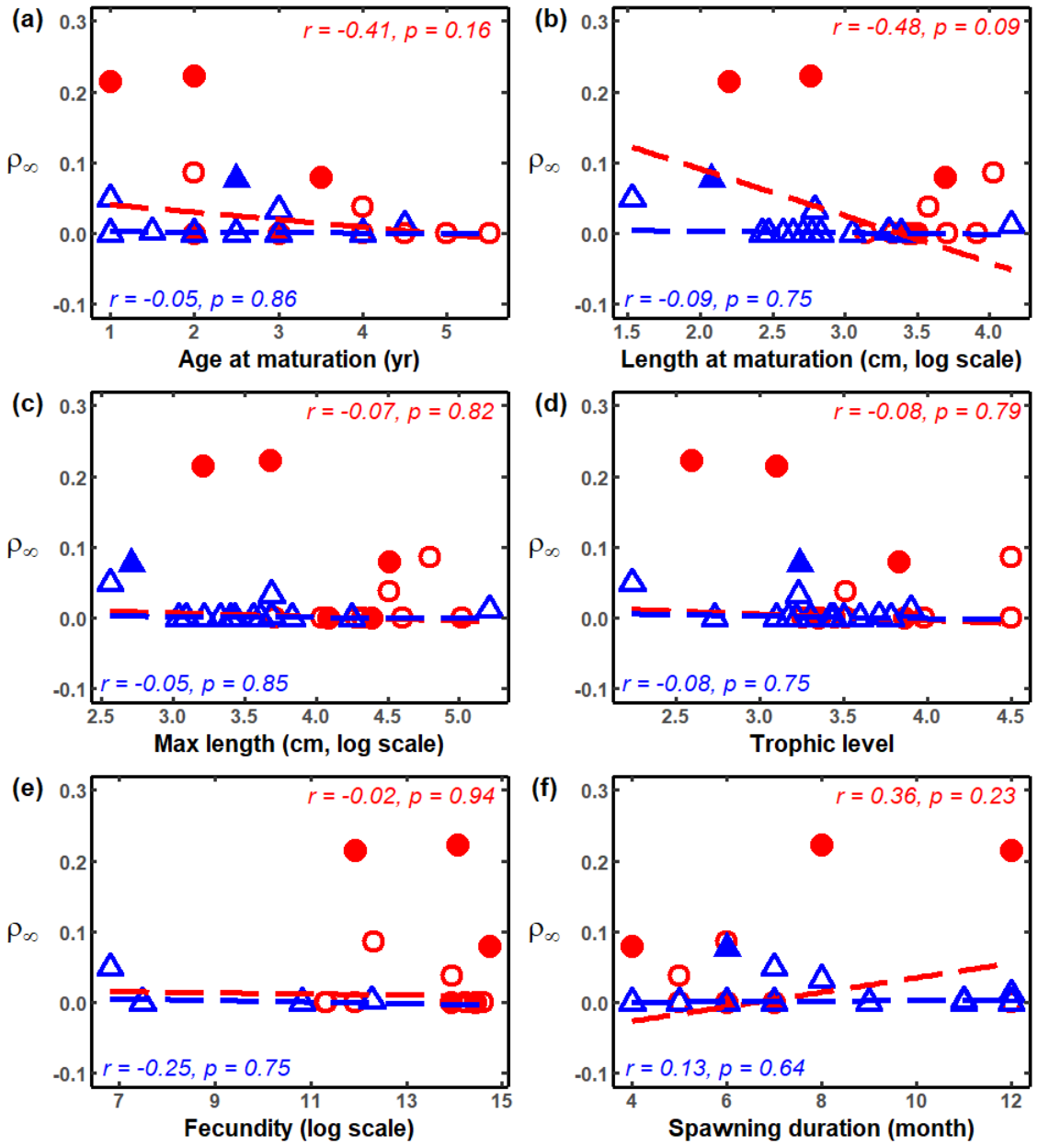

Figure S5. ρ_{∞} of exploited and unexploited species versus life-history traits. Red circles represent exploited species; blue triangles represent unexploited species; solid form represents complete synchrony decay pattern; hollow form represents incomplete synchrony decay pattern. Weighted least square was applied to describe the relationship between the two variables; weighted correlation coefficient and p-value for each trait is showed in the corner.

doi:10.6342/NTU202301753

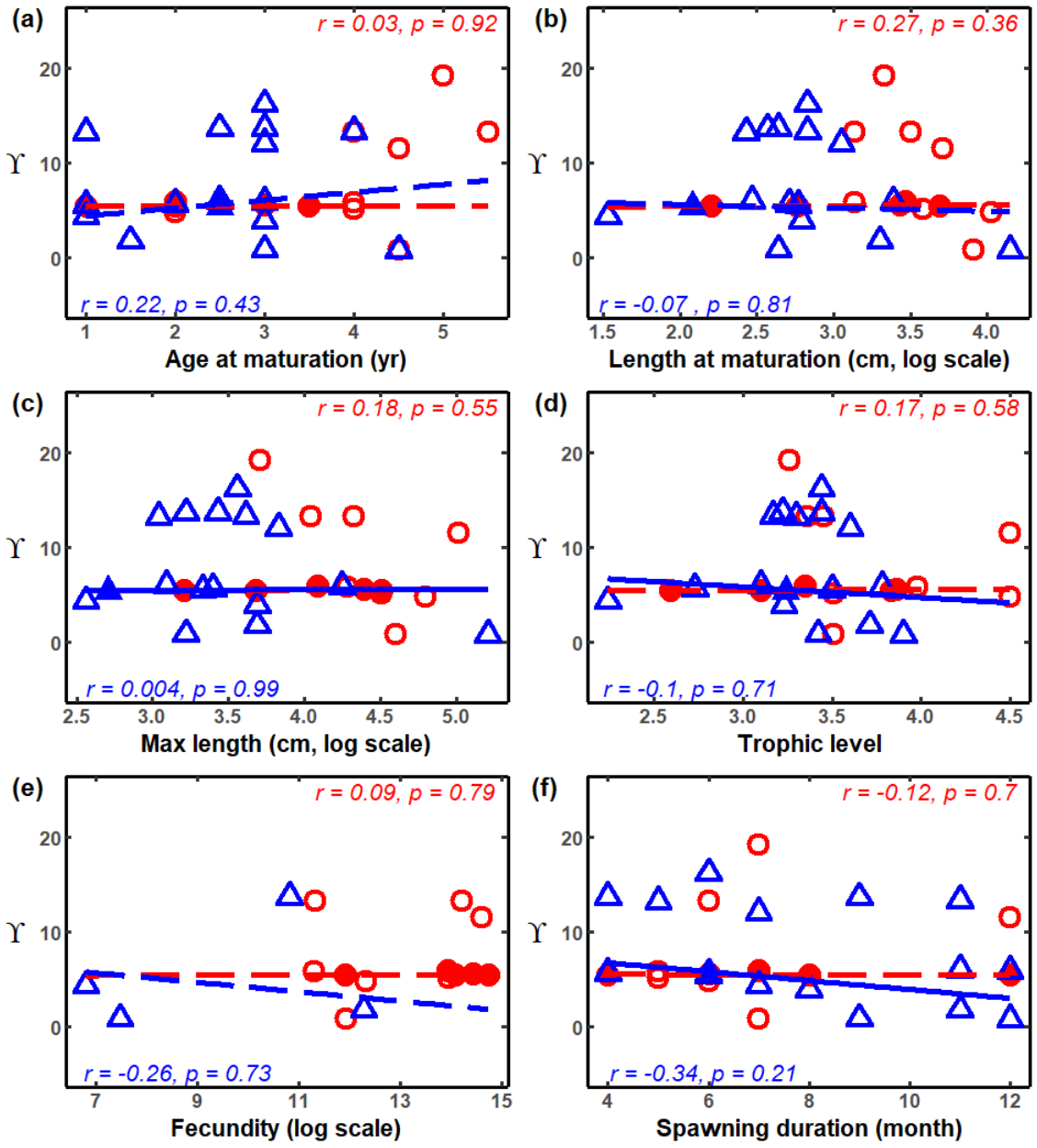

Figure S6. γ of exploited and unexploited species versus life-history traits. Red circles represent exploited species; blue triangles represent unexploited species; solid form represents complete synchrony decay pattern; hollow form represents incomplete synchrony decay pattern. Weighted least square was applied to describe the relationship between the two variables; weighted correlation coefficient and p-value for each trait is showed in the corner.

doi:10.6342/NTU202301753

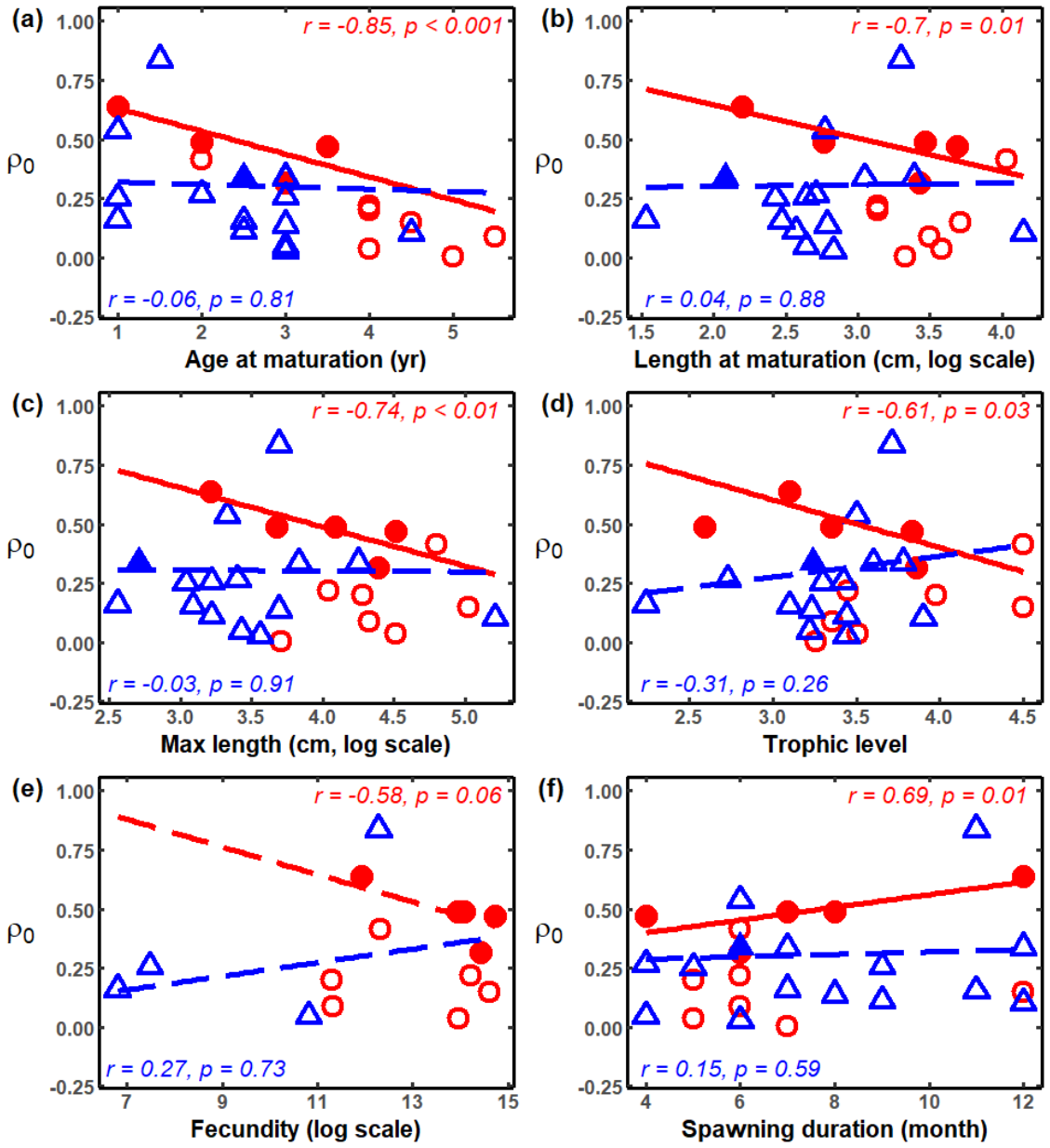

Figure S7. ρ_0 of exploited and unexploited species versus life-history traits during the cold climate period. Red circles represent exploited species; blue triangles represent unexploited species; solid form represents complete synchrony decay pattern; hollow form represents incomplete synchrony decay pattern. Weighted least square was applied to describe the relationship between the two variables; weighted correlation coefficient and p-value for each trait is showed in the corner.

doi:10.6342/NTU202301753

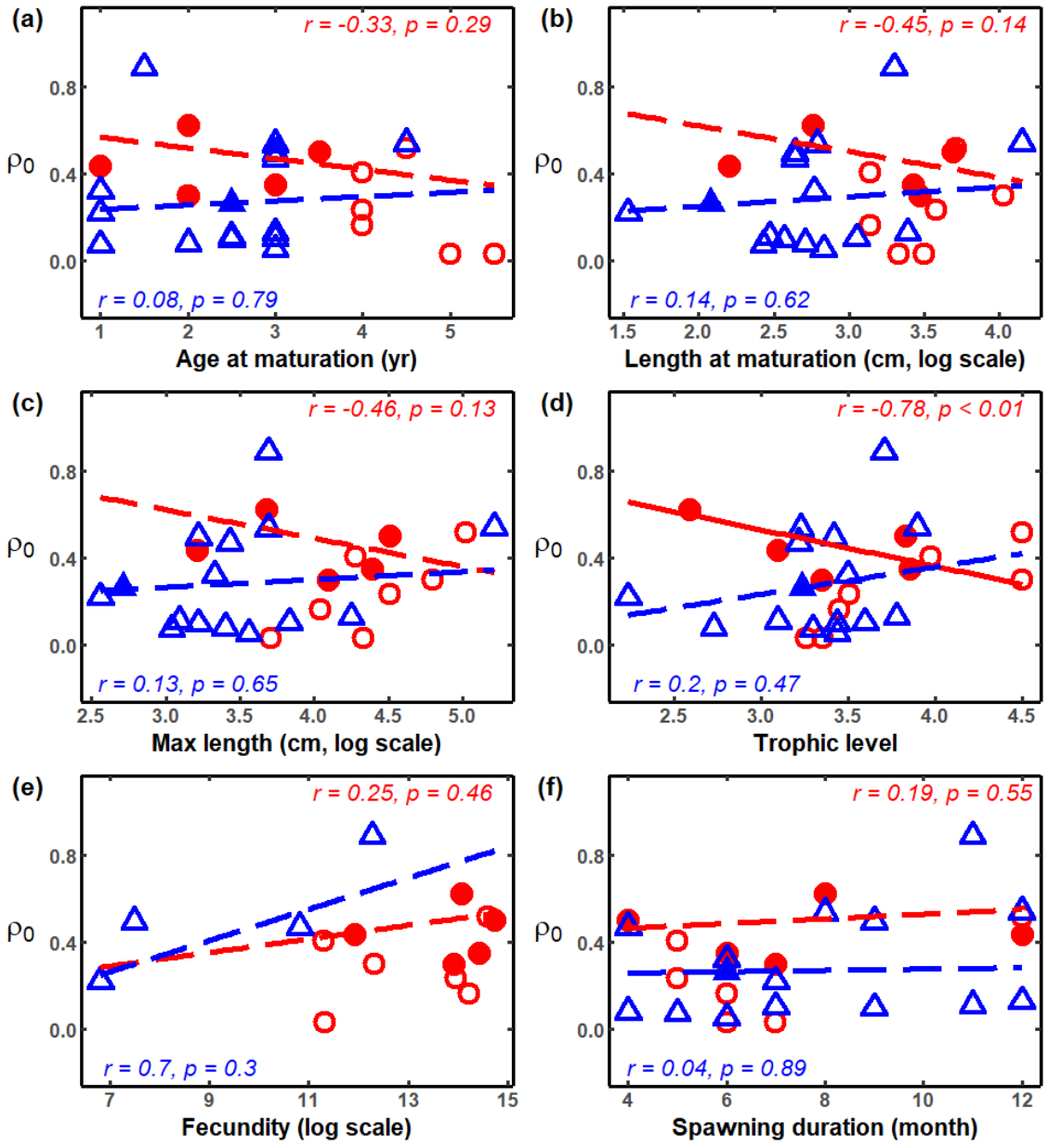

Figure S8. ρ_0 of exploited and unexploited species versus life-history traits during the warm climate period. Red circles represent exploited species; blue triangles represent unexploited species; solid form represents complete synchrony decay pattern; hollow form represents incomplete synchrony decay pattern. Weighted least square was applied to describe the relationship between the two variables; weighted correlation coefficient and p-value for each trait is showed in the corner.

doi:10.6342/NTU202301753

doi:10.6342/NTU202301753

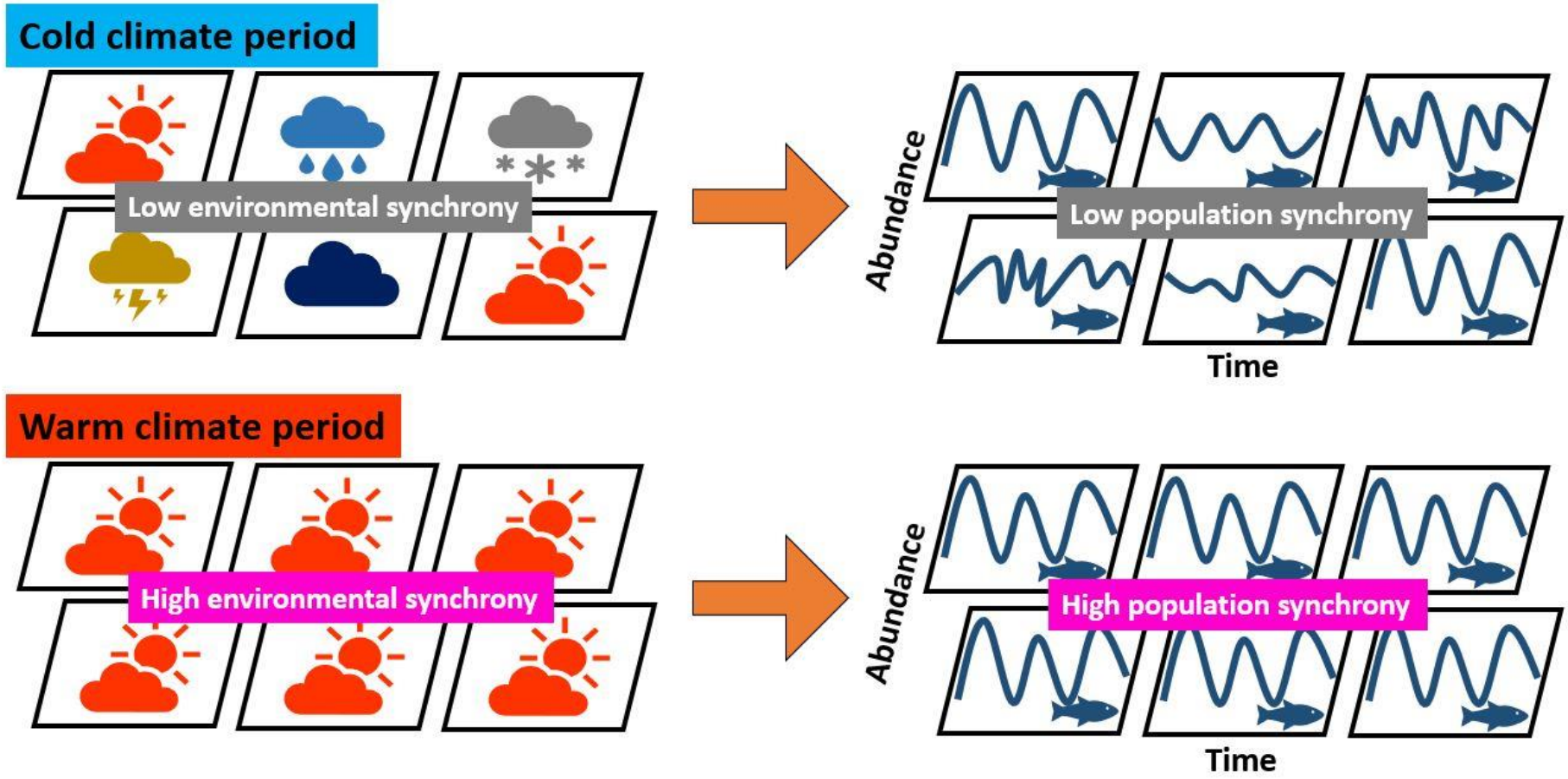

Figure S9. Illustration of spatial synchrony between environment and population during the warm and the cold climate period

doi:10.6342/NTU202301753

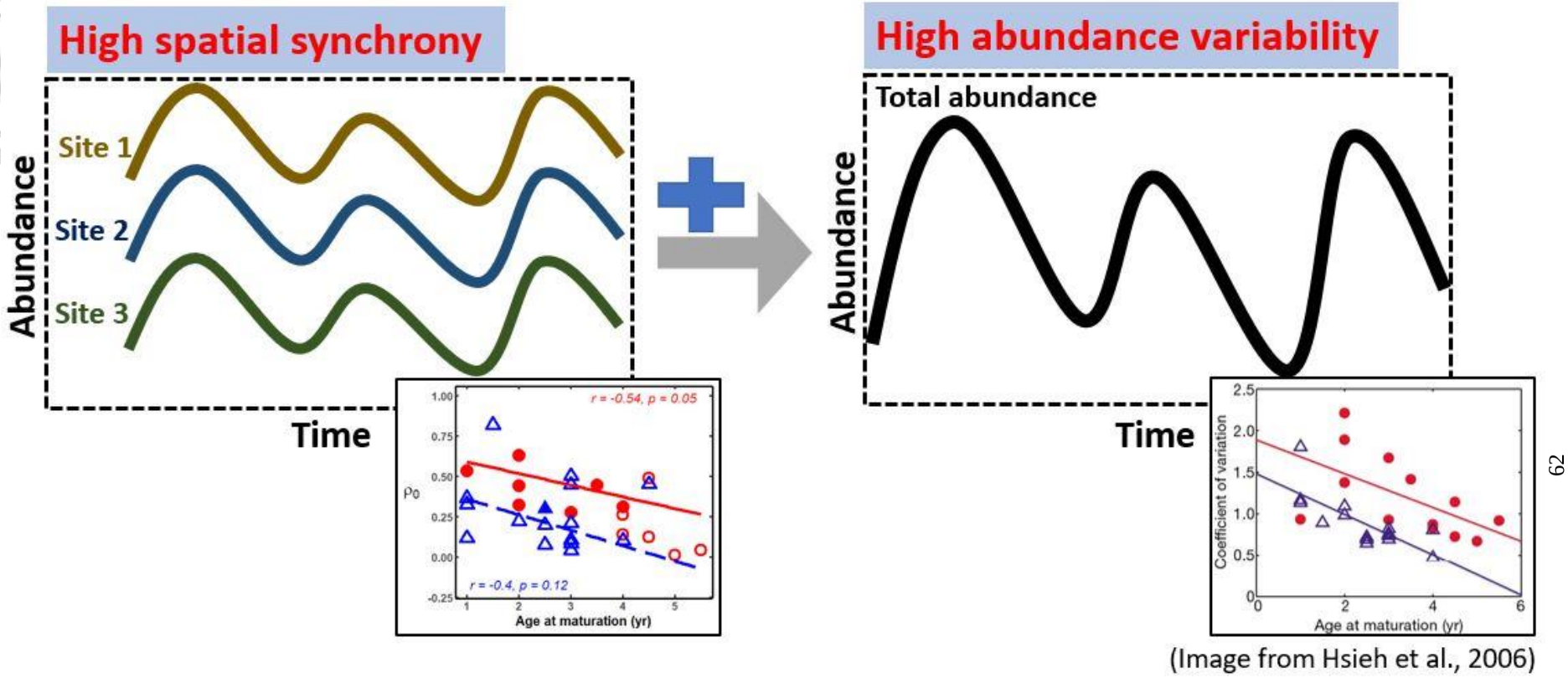

Figure S10. Illustration of how spatial synchrony leads to high temporal variability in abundance

doi:10.6342/NTU202301753

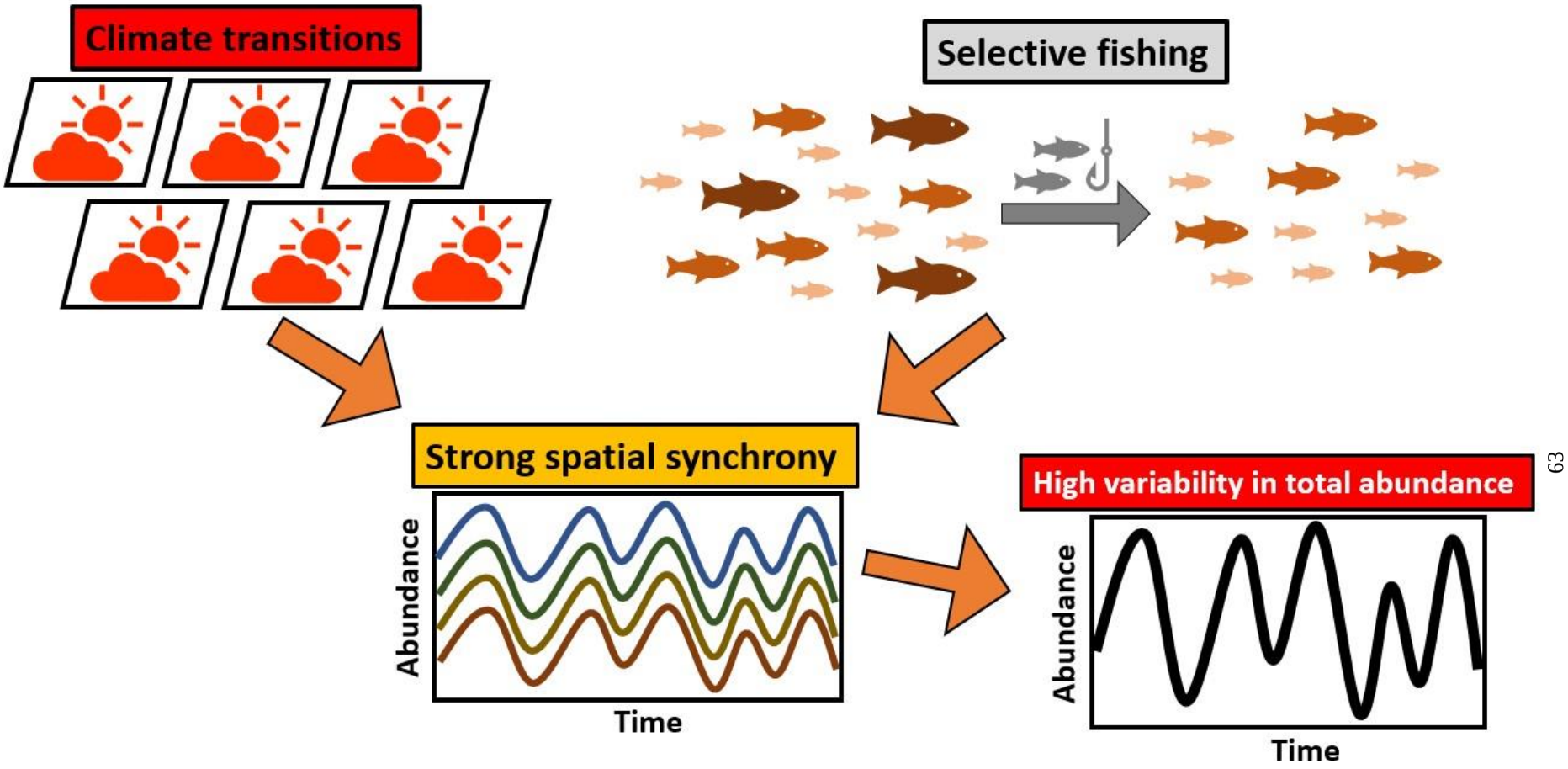

Figure S11. Diagram summarizing climate transitions and fishing can lead to high spatial synchrony, thereby causing high variability in total abundance, ultimately, increasing species' extinction risk.

Table S1. life-history traits for each species.

Species	Age at maturation	Length at maturation	Maximum length	Trophic level	Fecundity	Spawning duration
Engraulis mordax	1.00	2.20	3.21	3.10	11.92	12.00
Merluccius productus	3.50	3.69	4.51	3.83	14.73	4.00
Microstomus pacificus	5.50	3.50	4.33	3.36	11.33	6.00
Paralabrax clathratus	4.00	3.14	4.28	3.98	11.30	5.00
Paralichthys californicus	4.50	3.71	5.02	4.50	14.60	12.00
Parophrys vetulus	4.00	3.14	4.04	3.45	14.22	6.00
Sardinops sagax	2.00	2.76	3.68	2.59	14.08	8.00
Scomber japonicus	2.00	3.47	4.09	3.35	13.93	7.00
Scorpaenichthys marmoratus	4.50	3.91	4.60	3.51	11.93	7.00
Sebastes aurora	5.00	3.33	3.71	3.26	NA	7.00
Sebastes paucispinis	4.00	3.58	4.51	3.51	13.96	5.00
Sphyraena argentea	2.00	4.03	4.80	4.50	12.32	6.00
Trachurus symmetricus	3.00	3.43	4.39	3.86	14.43	6.00
Argentina sialis	2.50	2.47	3.09	3.10	NA	11.00
Chromis punctipinnis	2.00	2.71	3.40	2.73	NA	4.00
Cololabis saira	1.50	3.30	3.69	3.71	12.28	11.00
Hippoglossina stomata	3.00	2.79	3.69	3.23	NA	8.00
Hypsoblennius jenkins	1.00	1.53	2.56	2.24	6.80	7.00
Icichthys lockingtoni	3.00	3.05	3.83	3.60	NA	7.00
Leuroglossus stilbius	2.50	2.08	2.71	3.24	NA	6.00
Lyopsetta exilis	3.00	2.83	3.56	3.44	NA	6.00
Ophidion scrippsae	1.00	2.77	3.33	3.50	NA	6.00
Oxylebius pictus	3.00	2.64	3.22	3.42	7.48	9.00
Pleuronichthys verticalis	4.00	2.83	3.613	3.17	NA	11.00
Sebastes jordani	3.00	2.64	3.43	3.22	10.82	4.00
Symphurus atricaudus	1.00	2.43	3.04	3.30	NA	5.00
Tetragonurus cuvieri	3.00	3.39	4.25	3.78	NA	12.00
Trachipterus altivelis	4.50	4.15	5.21	3.90	NA	12.00
Zaniolepis frenata	2.50	2.57	3.22	3.44	NA	9.00

doi:10.6342/NTU202301753

Table S2. Exploited and unexploited species categories for each species.

Species	Common name	Status
Engraulis mordax	Northern anchovy	Exploited species
Merluccius productus	Pacific hake	Exploited species
Microstomus pacificus	Dover sole	Exploited species
Paralabrax clathratus	Kelp bass	Exploited species
Paralichthys californicus	California halibut	Exploited species
Parophrys vetulus	English sole	Exploited species
Sardinops sagax	Pacific sardine	Exploited species
Scomber japonicus	Pacific chub mackerel	Exploited species
Scorpaenichthys marmoratus	Cabezon	Exploited species
Sebastes aurora	Aurora rockfish	Exploited species
Sebastes paucispinis	Bocaccio	Exploited species
Sphyraena argentea	Pacific barracuda	Exploited species
Trachurus symmetricus	Jack mackerel	Exploited species
Argentina sialis	Pacific argentine	Unexploited species
Chromis punctipinnis	Blacksmith	Unexploited species
Cololabis saira	Pacific saury	Unexploited species
Hippoglossina stomata	Bigmouth sole	Unexploited species
Hypsoblennius jenkinsi	Mussel blenny	Unexploited species
Icichthys lockingtoni	Medusafish	Unexploited species
Leuroglossus stilbius	California smoothtongue	Unexploited species
Lyopsetta exilis	Slender sole	Unexploited species
Ophidion scrippsae	Basketweave cusk-eel	Unexploited species
Oxylebius pictus	Painted greenling	Unexploited species
Pleuronichthys verticalis	Hornyhead turbot	Unexploited species
Sebastes jordani	Shortbelly rockfish	Unexploited species
Symphurus atricaudus	California tonguefish	Unexploited species
Tetragonurus cuvieri	Smalleye squaretail	Unexploited species
Trachipterus altivelis	King-of-the-salmon	Unexploited species
Zaniolepis frenata	Shortspine combfish	Unexploited species

doi:10.6342/NTU202301753

Table S3. Ecological traits for each species.

Species	Habitat	Region	Spawning mode
Engraulis mordax	Water	Wide	Planktonic
Merluccius productus	Water	Wide	Planktonic
Microstomus pacificus	Soft	Cool	Planktonic
Paralabrax clathratus	Kelp	Warm	Planktonic
Paralichthys californicus	Soft	Warm	Planktonic
Parophrys vetulus	Soft	Cool	Planktonic
Sardinops sagax	Water	Warm	Planktonic
Scomber japonicus	Water	Warm	Planktonic
Scorpaenichthys marmoratus	Kelp	Cool	Demersal
Sebastes aurora	Soft	Cool	Live-bearer
Sebastes paucispinis	Water	Cool	Live-bearer
Sphyraena argentea	Water	Warm	Planktonic
Trachurus symmetricus	Water	Wide	Planktonic
Argentina sialis	Water	Wide	Planktonic
Chromis punctipinnis	Kelp	Warm	Demersal
Cololabis saira	Water	Wide	Planktonic
Hippoglossina stomata	Soft	Warm	Planktonic
Hypsoblennius jenkinsi	Kelp	Warm	Demersal
Icichthys lockingtoni	Water	Wide	Planktonic
Leuroglossus stilbius	Water	Wide	Planktonic
Lyopsetta exilis	Soft	Cool	Planktonic
Ophidion scrippsae	Soft	Warm	Planktonic
Oxylebius pictus	Kelp	Cool	Demersal
Pleuronichthys verticalis	Soft	Warm	Planktonic
Sebastes jordani	Water	Cool	Live-bearer
Symphurus atricaudus	Soft	Warm	Planktonic
Tetragonurus cuvieri	Water	Wide	Planktonic
Trachipterus altivelis	Water	Wide	Planktonic
Zaniolepis frenata	Soft	Wide	Live-bearer

doi:10.6342/NTU202301753